

Research article

Heterogeneous impacts of human activities and climate change on transformed vegetation dynamics on the Qinghai-Tibet Plateau



Dazhi Yang ^{a,b} , Yaqun Liu ^{a,*}

^a Institute of Geographic Sciences and Natural Resources Research, Chinese Academy of Sciences, Beijing, 100101, China

^b College of Resources and Environment, University of Chinese Academy of Sciences, Beijing, 100049, China

ARTICLE INFO

Keywords:

Qinghai-Tibet plateau
Vegetation
Driving factors
Transition type
GNDVI
Human activities

ABSTRACT

In the context of intensifying global environmental change, elucidating vegetation dynamics and their driving mechanisms is vital for sustainable ecosystem management. The Qinghai-Tibet Plateau (QTP), a region known for its sensitivity and vulnerability, exhibits a high degree of responsiveness to climate change and human activities. The region's pronounced spatiotemporal heterogeneity renders it an optimal area for investigating vegetation changes and their driving mechanisms. However, existing research predominantly emphasizes natural factors, with insufficient systematic analysis of human activities, thereby constraining a comprehensive understanding of driving mechanisms. This study utilizes MODIS NDVI data to systematically analyze GNDVI (the average NDVI during the growing season) trends and their driving mechanisms across the QTP from 2000 to 2018, integrating natural factors (temperature, precipitation, potential evapotranspiration, snow depth, elevation, slope) and human factors (roads, population, grazing intensity) from multi-scale and vegetation-type perspectives. Results reveal a significant increasing trend in GNDVI ($p < 0.05$) across the QTP, with pronounced improvements in the northeast and degradation in specific regions of the southwest and southeast. From 2000 to 2018, 79.19% of QTP vegetation exhibited improvement (39.52% significantly), while 14.28% experienced degradation (2.78% significantly). During the study period, the QTP climate exhibited a warming and moistening trend, which generally benefited vegetation growth. The impacts of natural and human factors on vegetation changes vary significantly across different spatial regions. Population density and grazing intensity have obvious threshold effects on vegetation dynamics: when population density exceeds 17 pop/km², their effects on vegetation change rate approach marginal effects, while grazing intensity exceeds 250 SU/km², resulting in a significant decrease in GNDVI change rate. Notably, grazing and tourism activities near roads and lakes negatively impacted GNDVI in the southwest and southeast, partially offsetting the positive effects of climate change and contributing to degradation. Based on these findings, the study recommends establishing a long-term investment mechanism for ecosystem protection, implementing differentiated regional management strategies, and enhancing regulatory oversight of human activities. Specifically, strict controls on grazing and tourism development in ecologically sensitive areas are necessary to mitigate their impacts on fragile ecosystems. This study constructs a framework that integrates the spatiotemporal heterogeneity of natural and human factors, overcoming the limitations of traditional methods. It advances the theoretical understanding of the driving mechanisms behind vegetation dynamics in alpine ecosystems and provides a scientific foundation for formulating differentiated ecological protection policies and sustainable management strategies.

1. Introduction

Vegetation, as a core component and primary producer within terrestrial ecosystems, plays a crucial role in mediating the interactions between abiotic environmental factors such as water, soil, and

atmosphere, and biotic components including animals and microorganisms (Liu et al., 2015; Thompson et al., 2025). By regulating global biogeochemical processes such as the water cycle, carbon cycle, and energy exchange, vegetation provides essential ecological products and services that support socio-economic systems (Zhang et al., 2017b; Pan

* Corresponding author. Key Laboratory of Regional Sustainable Development Modeling, Institute of Geographic Sciences and Natural Resources Research, Chinese Academy of Sciences, No. 11(A), Datun Road, Chaoyang District, Beijing, 100101, China.

E-mail address: liuyaqun@igsnrr.ac.cn (Y. Liu).

et al., 2018; Xiao et al., 2023). In recent years, with the intensification of global environmental change (Zhang et al., 2022; Adeyeri et al., 2024), the dynamics of vegetation have become a focal point of research in fields such as climate change, ecosystem services, land use/land cover, and land degradation (Forzieri et al., 2017; Idusseri et al., 2024; Li et al., 2024). In this context, a deeper understanding of the characteristics of vegetation dynamics and their driving mechanisms is crucial for predicting, adapting to, and mitigating the impacts of global environmental change, as well as for achieving sustainable ecosystem management.

NDVI, one of the most widely used vegetation indices in research, is highly correlated with key vegetation parameters such as Net Primary Productivity (NPP), photosynthetic capacity, vegetation cover, and Leaf Area Index (LAI) (Fensholt et al., 2004; Anees et al., 2024; Zarei et al., 2024). The long-term NDVI datasets obtained through remote sensing technology provide critical evidence for studying vegetation growth responses to global environmental changes (Gutiérrez-Hernández et al., 2025). Currently, commonly used long-term NDVI datasets include GIMMS-NDVI3g (1981–2015), SPOT-VEG (1998–2014), and MODIS (2000–present) (Liu et al., 2023). Numerous studies have shown that vegetation “greening” trends (i.e., increased NDVI) have generally occurred globally over the past few decades, particularly in high-latitude regions of the Northern Hemisphere (Rogier et al., 2011; Recuero et al., 2019; Jeong et al., 2024; Zhou et al., 2024). These findings have been corroborated by ground vegetation survey data and ecosystem model simulations (Khormizi et al., 2023; Yan et al., 2024). However, different NDVI products exhibit significant differences in revealing spatial patterns and magnitudes of vegetation greening or browning trends. For example, inconsistencies in GIMMS-NDVI3g and SPOT-VEG data due to sensor changes may lead to discrepancies, while MODIS V5 has introduced biases in the trends of NDVI decline in tropical regions due to sensor performance degradation (Panigrahi et al., 2021). In contrast, MODIS V6, with improved calibration algorithms, has significantly reduced sensor degradation impacts and is widely regarded as a more reliable dataset for vegetation dynamics research (Giglio et al., 2018). Therefore, studies based on MODIS NDVI-V6 data can more accurately reflect vegetation dynamics.

The trends in NDVI result from the combined effects of natural and anthropogenic driving factors. However, attributing these trends to specific driving mechanisms remains a significant challenge, primarily due to spatial heterogeneity, temporal dynamics, and complex interactions of these factors (Wen et al., 2017; Han and Song, 2022; Chen et al., 2024). Regarding natural factors, global warming has significantly promoted greening trends in high-latitude and high-altitude regions by enhancing vegetation photosynthesis and extending the growing season (Wu et al., 2015). Precipitation, on the other hand, is the dominant limiting factor for vegetation growth in arid and semi-arid regions. Conversely, droughts and wildfires triggered by warming or reduced precipitation have become major natural drivers of vegetation browning (Pontes-Lopes et al., 2021). Additionally, increased CO₂ concentrations have generally promoted vegetation growth through the fertilization effect (Wang et al., 2020). Large-scale climatic events such as El Niño phenomena and volcanic eruptions alter temperature, precipitation, atmospheric composition, and radiation conditions, leading to regional greening or browning of vegetation (Tortini et al., 2017; Yan et al., 2021). On the anthropogenic side, land protection, irrigation, and fertilization management practices typically promote vegetation greening. In contrast, human activities such as deforestation, overgrazing, and slope cultivation have significant negative impacts on vegetation growth (McNicol et al., 2023).

While existing studies have highlighted the importance of the aforementioned driving factors, significant gaps remain in current research under the Anthropocene. Firstly, most studies predominantly focus on natural factors, with relatively insufficient systematic analysis of human activities (Piao et al., 2020). Although a few studies have attempted to quantify the effects of climate change and land use on vegetation growth (Shen et al., 2023), they often overlook the integrated

influence of other critical natural factors (such as topography, vegetation types, and climatic zones) and human factors (such as population density, GDP, and grazing intensity). Secondly, the driving mechanisms of vegetation growth vary significantly across spatial scales and vegetation types, and these mechanisms evolve dynamically over time. Previous studies, however, have generally lacked systematic analysis from a multi-scale and vegetation-type-specific perspective. Additionally, the interactions between natural and anthropogenic factors and their relative contributions to vegetation dynamics remain unclear, limiting a comprehensive understanding of the driving mechanisms of vegetation change. Therefore, to address global environmental changes and achieve sustainable ecosystem management, there is an urgent need to conduct systematic research on NDVI trends and their driving mechanisms across multiple scales, from pixels to regions, and across different vegetation types. By integrating multi-source data and analytical methods, it is essential to accurately reveal the complexity of vegetation dynamics, thus providing scientific support for addressing global environmental changes.

The Qinghai-Tibet Plateau (QTP) is a crucial component of Earth's system, often referred to as the “Third Pole” and “Asia’s Water Tower.” As the largest high-altitude region globally, it plays a vital role in storing biodiversity, water resources, and climate-driven gases. Its impact on the regulation of global climate and water resources is indispensable, making it a critical biophysical entity (Ehlers et al., 2022; Miao et al., 2024). Since 1980, the temperature of the QTP has risen at a rate of 0.35 °C per decade, accompanied by a yearly increase in evapotranspiration, with an annual rise of 9 mm per decade (Li et al., 2025). Research has shown that the QTP’s unique geo-atmospheric coupling system, along with the interaction between the troposphere and stratosphere, amplifies its influence on regional and global climates through cascading effects and remote coupling mechanisms (You et al., 2021), which have been particularly significant in regulating monsoon circulation, precipitation patterns, and phenomena such as the El Niño-Oscillation (Yao et al., 2019; Yu et al., 2022; Wu et al., 2023). However, the QTP is also regarded as one of the most ecologically vulnerable regions, with its unique environmental conditions making it highly sensitive to both climate change and human activities (Wang et al., 2011). Vegetation, as a key component of land cover, is one of the most sensitive biological indicators of environmental changes, and its phenology and distribution patterns have been in dynamic flux over time (Shen et al., 2015). Therefore, vegetation is often a central focus of environmental change monitoring. Climate changes, such as the significant warming and shifts in moisture patterns experienced on the QTP over the past fifty years, have deeply influenced the spatiotemporal distribution of vegetation (Lu et al., 2023a, 2024). Meanwhile, overgrazing and tourism activities have caused localized vegetation degradation, while ecological protection initiatives by the Chinese government, such as grazing bans and ecological compensation programs, have significantly improved vegetation cover and productivity. As a result, vegetation change exhibits pronounced spatial heterogeneity, and the interplay of natural and anthropogenic driving factors has led to complex ecological response patterns (Yao et al., 2022; Degen, 2025). However, there remains a lack of systematic understanding of the spatiotemporal patterns of vegetation change, the distribution of degraded areas, and the spatiotemporal heterogeneity of driving mechanisms on the QTP. This gap hinders a deeper understanding of ecosystem evolution patterns and the optimization of ecological protection policies.

To address this, our study systematically analyzes the multi-scale characteristics of vegetation cover change on the QTP from 2000 to 2018 using MODIS NDVI-C6 data. We integrate natural factors (such as temperature, precipitation, elevation, and slope) and human factors (such as road, population distribution, and grazing intensity) to uncover the driving mechanisms of vegetation change and their spatiotemporal heterogeneity. The aim is to provide a scientific basis for the protection and sustainable development of the plateau’s ecosystems. The specific

objectives of the study include: (1) Quantitatively characterizing the spatiotemporal trends and spatial differentiation features of GNDVI (the average NDVI during the growing season) on the QTP from 2000 to 2018 at multiple scales, including pixel, ecological zone, and vegetation type perspectives. (2) Elucidating the driving mechanisms of GNDVI change by natural and human factors and explaining their spatiotemporal heterogeneity patterns. The findings of this research will offer critical theoretical support and practical guidance for formulating differentiated ecological protection policies and adaptive management strategies on the QTP.

2. Materials

2.1. Study area

The QTP located in the southwest of China, is the highest geographical unit globally, with an average elevation exceeding 4000 m and a total area of approximately 2.58×10^8 ha. With increasing altitude and latitude, the annual average temperature in this area shows a significant gradient change, from above 15 °C in the southeast to below 0 °C in the northwest. A warming trend of 0.42 °C per decade—more than twice the global average (Yao et al., 2019)—driven by both natural and anthropogenic factors, underscores the region's ecological sensitivity. Precipitation also varies significantly, with annual averages exceeding 1000 mm in the southeast and falling below 50 mm in the northwest, creating a mosaic of ecosystems ranging from subtropical rainforests to grasslands and deserts. This spatial heterogeneity makes the QTP one of the most biologically diverse regions worldwide (Fig. 1). Grassland ecosystems dominate the plateau, occupying over 60% of its total area. However, decades of global warming and intensified human activity have led to severe grassland degradation, posing a significant threat to the region's ecological sustainability (Degen, 2025). In response, the Chinese government has implemented a series of ecological protection measures since the late 20th century, including grazing bans, grassland restoration projects, ecological subsidies, and the

establishment of nature reserves. These efforts have effectively safeguarded the ecological security of the plateau, leading to overall environmental improvements. However, grassland degradation persists in areas with intense human activity. Currently, human activities such as grazing, cultivation, infrastructure development, and tourism are concentrated in the more densely populated eastern and southern regions. In contrast, the sparsely inhabited northwest, often called "no-man's-land," remains relatively undisturbed (Fig. 1).

2.2. Data sources

The data used in this study primarily include NDVI data, natural factor data, and human factor data.

(1) NDVI time series data

The NDVI data for the period 2000–2018 were sourced from the MODIS MOD13A3 v601 (NDVI-V6.1) product (USGS, 2020), to analyze trends in vegetation growth. The NDVI-V6 product, with a spatial resolution of 1 km and a monthly temporal resolution, is derived from the weighted temporal average of the 16-day product. This product significantly mitigates the effects of sensor degradation and cloud contamination, with its algorithm further optimized. Consequently, compared to GIMMS-NDVI3g, SPOT-VEG, and NDVI-V5, NDVI-V6 has emerged as a more reliable NDVI dataset for current research. This study used GNDVI, the average NDVI during the growing season (May–October), to more accurately reflect vegetation growth conditions. Areas with annual maximum NDVI values below 0.01, considered non-vegetated, were masked.

(2) Natural factors

The climatic data for the period 2000–2018, including annual precipitation and annual mean temperature, were derived from ground observations at over 300 meteorological stations across the QTP and its

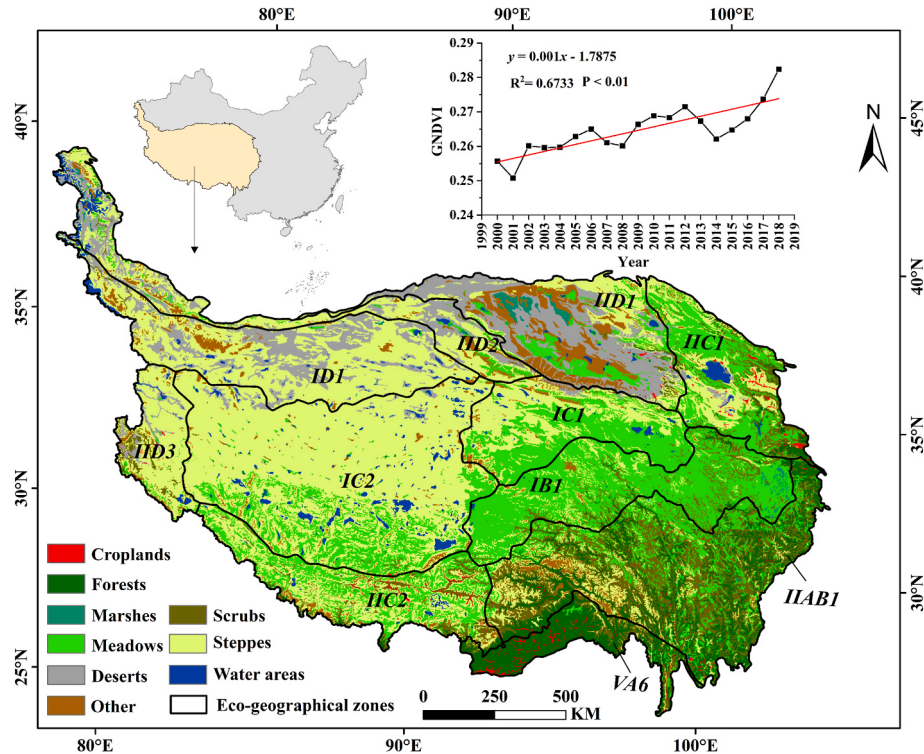


Fig. 1. The geographical location, vegetation types, eco-geographical regions and average annual GNDVI fitting trend of the Qinghai-Tibet Plateau.

surrounding areas (CMDSC, 2024). Firstly, monthly precipitation and monthly mean temperature were calculated for each year. Subsequently, using the thin plate spline method in ANUSPLIN software, elevation was introduced as a covariate to interpolate temperature and precipitation raster data at a 1 km resolution. Annual and growing season temperature and precipitation data are synthesized from monthly data.

The potential evapotranspiration data are sourced from the Tibetan Plateau Data Center (TPDC, 2024), with monthly potential evapotranspiration values at a resolution of 1 km. Additionally, daily snow depth data are also provided by the same center, with a resolution of 0.05°. By applying temporal filtering, projection, resampling, and raster computation, annual and growing season evapotranspiration and snow depth data for the Tibetan Plateau from 2000 to 2018 were derived, with a final resolution of 1 km.

Elevation data were sourced from the 30m resolution ASTER GDEM dataset (NASA, 2015), and slope was calculated. To match the resolution of NDVI, the 30m elevation and slope datasets were resampled to 1 km using block mean statistics.

The vegetation type data were derived from the 1:1 million Chinese Vegetation Type Spatial Distribution dataset (RESDP, 2024), provided as 1 km raster data.

(3) Human factors

The 1000m resolution population data for the period from 2000 to

2018 were sourced from the WorldPop dataset (WorldPop, 2019). This dataset spatially allocates statistical population data using machine learning algorithms, considering factors such as land use/cover, nighttime light imagery, and residential point density. The WorldPop dataset is openly available under the Creative Commons Attribution 4.0 International License (CC BY 4.0), which allows for free use, distribution, and adaptation of the data, provided that proper attribution is given to the original source.

The livestock breeding quantity data for Qinghai and Tibet from 2000 to 2018 were sourced from the China Statistical Yearbook, with statistical units at the county level. The data were standardized using sheep units, with large livestock (e.g., cattle and horses) converted at a rate of 4.5 sheep units.

The grazing intensity data for the Tibetan Plateau from 2000 to 2018 were derived from the study by Zhou et al. (2024), with the dataset titled "Gridded Dataset of Grazing Intensity." The data were generated using machine learning techniques and represents grazing intensity at the grid scale in standard sheep units, with a resolution of 100 m. In this study, the data was preprocessed and aggregated to a 1 km resolution grid.

The road network and rivers/lakes distribution vector data for the QTP in 2018 were sourced from the OSM road network (OSM, 2019). OpenStreetMap data are licensed under the Open Data Commons Open Database License (ODbL). In this study, distance to road and distance to river were calculated using the Euclidean distance method at a 1 km resolution.

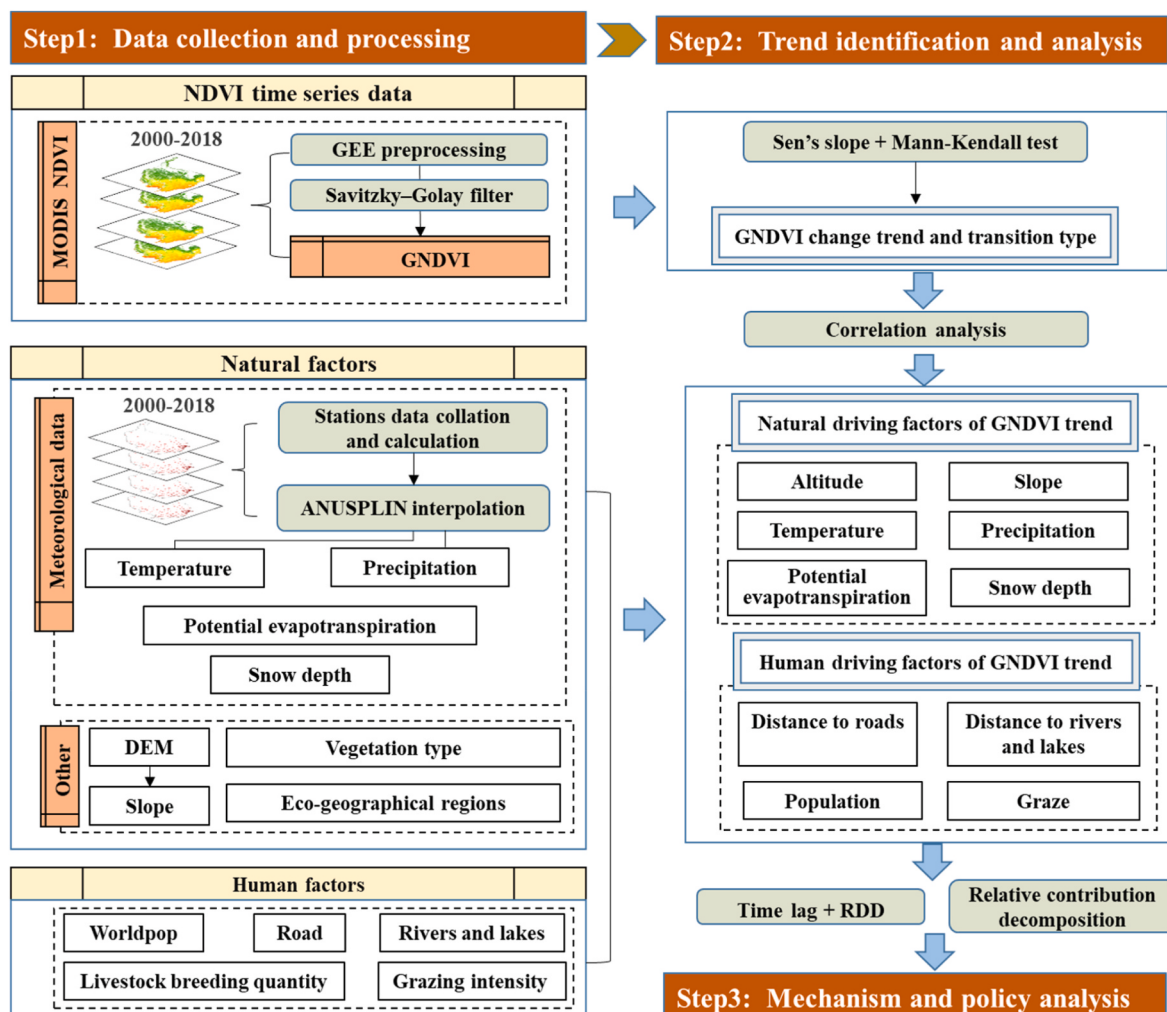


Fig. 2. Research framework.

3. Methods

In this study, we begin by collecting and processing the data (Fig. 2). Using the Google Earth Engine (GEE) platform, we processed MODIS data, applying Savitzky–Golay filtering for smoothing to obtain a long-term time series of GNDVI data. At the same time, we collected and processed data on natural factors (including Precipitation, Temperature, Potential evapotranspiration, Snow depth, DEM, Vegetation type, and Eco-geographical regions) as well as human factors (including World-pop, Road, Rivers and lakes, Livestock breeding quantity, Grazing intensity). Next, we performed trend identification and analysis. Using the Sen's slope and Mann-Kendall test methods, we analyzed the multi-scale trends of GNDVI from 2000 to 2018 at the pixel, eco-geographical region, and regional levels. Based on the segmented trend changes between 2000–2009 and 2009–2018, we identified the types of GNDVI changes. Furthermore, we conducted correlation analysis by combining the data and trends of various factors to explore the natural and human driving factors behind the GNDVI trend changes. We further conducted a time-lag analysis, RDD (regression discontinuity design), and relative contribution decomposition. Finally, based on the trend analysis, change types, and threshold characteristics of the driving factors, we explored the mechanisms of vegetation change and conducted relevant policy analysis.

3.1. Analysis of change trends

The Slope method, based on linear regression, is widely used for analyzing trends in time series data (Lavagnini et al., 2011). In this study, we used the least squares method to calculate the Slope, allowing for the quantification of interannual trends in GNDVI, climatic factors over different periods (2000–2018, 2000–2009, and 2009–2018). A positive Slope (Slope > 0) indicates an increasing trend, while a negative Slope (Slope < 0) indicates a decreasing trend. The formula is:

$$\text{Slope} = \frac{n \times \sum_{i=1}^n (i \times V_i) - \sum_{i=1}^n i \times \sum_{i=1}^n V_i}{n \times \sum_{i=1}^n i^2 - \left(\sum_{i=1}^n i \right)^2} \quad (1)$$

$$\text{Slope\%} = \frac{n \times \text{Slope}}{\sum_{i=1}^n V_i} \times 100 \quad (2)$$

Where the Slope represents the annual change in a variable V, and Slope % represents the annual change rate. V_i is the value of the variable in year i , and n is the total number of years. We abbreviate the Slope values for GNDVI, precipitation, and temperature as NS, PS, and TS, respectively. Their corresponding Slope% values are abbreviated as NS%, PS%, and TS%.

Previous studies have often considered an NDVI change rate less than $-0.05\%/\text{a}$ as indicative of degradation. In this study, GNDVI change levels are categorized into five grades—High Greening (HG), Low Greening (LG), High Browning (HB), Low Browning (LB), and Nonsignificant Change (NC)—based on thresholds of NS% values of -0.5 , -0.05 , 0.05 , and 0.5 .

$$x = \begin{cases} \text{High Greening, } NS\% > 0.5 \\ \text{Low Greening, } -0.05 \leq NS\% \leq 0.5 \\ \text{Nonsignificant Change, } -0.05 < NS\% < 0.05 \\ \text{Low Browning, } -0.5 \leq NS\% \leq -0.05 \\ \text{High Browning, } NS\% < -0.5 \end{cases} \quad (3)$$

3.2. Mann - Kendall test

The Mann-Kendall (MK) algorithm is a non-parametric statistical

method (Mann, 1945) for detecting trends in time series data. This method identifies the presence of upward or downward trends by comparing the sign differences between pairs of data points, without assuming any specific data distribution. As such, it is particularly effective for sequences exhibiting irregular fluctuations or non-normal distributions (Hamed, 2009). Furthermore, the Mann-Kendall method can be coupled with the Sen's Slope estimator to quantify the slope of the trend, offering robust quantitative insights into trend dynamics (Gocic et al., 2013; Güçlü, 2018). Due to these advantages, the Mann-Kendall algorithm has gained widespread attention and application in fields such as climate change and environmental monitoring (Yang et al., 2024; Lu et al., 2025).

In this test model, the null hypothesis (H_0) assumes that the time series data x_1, x_2, \dots, x_n (where n is the length of the dataset) are independently and randomly distributed. The alternative hypothesis (H_1) is a two-sided test, indicating that for all $i, j \leq n$, and $i \neq j$, the distributions of x_i and x_j are different. Based on this, the test statistic S is defined as:

$$S = \sum_{i=2}^n \sum_{j=1}^{i-1} \text{sign}(x_i - x_j) \quad (4)$$

Where S follows a normal distribution with a mean of 0. The sign function $\text{sign}(x_i - x_j)$ takes the value -1 , 0 , or 1 when $x_i - x_j$ is less than, equal to, or greater than 0, respectively.

The calculation of the M-K test statistic Z is given by:

$$Z = \begin{cases} (S - 1) / \sqrt{\text{Var}(S)} & S > 0 \\ 0 & S = 0 \\ (S + 1) / \sqrt{\text{Var}(S)} & S < 0 \end{cases} \quad (5)$$

$$\text{Var}(S) = \frac{n(n-1)(2n+5) - \sum_{i=1}^m t_i(t_i-1)(2t_i+5)}{18} \quad (6)$$

where n is the total number of data in the sequence, m is the number of groups of repeated data, and t_i is the number of occurrences of the i -th group of repeated data. In a two-sided trend test, for a given significance level α , the null hypothesis (H_0) is rejected if $|Z| \geq Z_{1-\alpha/2}$. This suggests a significant upward or downward trend in the time series at the α confidence level. When $Z > 0$, it indicates an upward trend, and when $Z < 0$, it indicates a downward trend.

3.3. Piecewise regression and classification of change types

Piecewise regression is a method that more accurately captures nonlinear trends in data (Yu et al., 2024). The core idea is to divide the data into multiple intervals, fit different regression models within each interval, and use breakpoints (i.e., inflection points) to reflect changes in the data structure. The main advantage of this approach is its ability to effectively handle datasets with different trends or clear inflection points, overcoming the limitation of traditional regression models that assume a single linear relationship. Especially when analyzing complex environmental, economic, or ecological data, piecewise regression can more precisely reveal the changing patterns at different stages, thereby enhancing understanding of the underlying mechanisms behind the data (Werner et al., 2015; Pan et al., 2018).

In this study, we divided the study period into 2000–2009 and 2009–2018 based on the approximate turning points of ecological protection projects and livestock quantity changes (Shao et al., 2022; Sun et al., 2022). Based on the annual GNDVI change rates for 2000–2009 (NS1%) and 2009–2018 (NS2%), the GNDVI trends were categorized into five types: Greening-Greening (GG), Browning-Greening (BG), Browning-Browning (BB), Greening-Browning (GB), and Nonsignificant Transition (NT).

$$TT = \begin{cases} \text{Greening - Greening, } (NS\% \geq 0.05) \text{ and } (NS2\% \geq 0.05) \\ \text{Browning - Greening, } (NS1\% \leq -0.05) \text{ and } (NS2\% \geq 0.05) \\ \text{Browning - Browning, } (NS1\% \leq -0.05) \text{ and } (NS2\% \leq -0.05) \\ \text{Greening - Browning, } (NS1\% \geq 0.05) \text{ and } (NS2\% \leq -0.05) \\ \text{Nonsignificant Transition, } (-0.05 < NS1\% < 0.05) \text{ or } (-0.05 < NS2\% < 0.05) \end{cases} \quad (7)$$

3.4. Linear correlation analysis

Simple linear correlation analysis is used to measure the strength and direction of correlation between two variables. In this study, the correlation coefficient R is applied to assess the relationships between climatic factors and vegetation changes (measured by GNDVI), and to analyze their spatial heterogeneity.

$$R_{xy} = \frac{\sum_{i=1}^n [(x_i - \bar{x})(y_i - \bar{y})]}{\sqrt{\sum_{i=1}^n (x_i - \bar{x})^2} \sqrt{\sum_{i=1}^n (y_i - \bar{y})^2}} \quad (8)$$

where R_{xy} represents the simple correlation coefficient between variables x and y , with a range of [-1, 1]. The closer the absolute value of R is to 1, the stronger the correlation. When R falls within [-0.3, 0.3] imply an insignificant correlation; values within [-1, -0.3] indicate a negative correlation, and those in [0.3, 1] indicate positive correlations. x_i and y_i are the values of variables x and y in year i , while \bar{x} and \bar{y} are their respective means over n years.

3.5. Time lag analysis of climatic factors

In this study, precipitation, temperature, potential evapotranspiration, and snow depth were selected as independent variables, while the GNDVI served as the dependent variable. The objective was to assess the dependence of GNDVI on these variables at different time-lag scales. According to existing literature, time lags typically range from 0 to several months, with a lag of one quarter (i.e., 3 months) being the most common (Qi et al., 2025). Therefore, this study considered time lags from 0 to 4 months and measured the relationships using correlation coefficients R_0, R_1, \dots, R_4 . For any given grid cell i , the peak correlation value R_{ij} (where $0 \leq j \leq 4$) was identified. The time-lag model is expressed as:

$$TL_i = j, \text{ when } R_{ij}^2 = \text{Max}\{R_0^2, R_1^2, \dots, R_4^2\} \quad (9)$$

where TL_i represents the lag time (month) of grid i , and j represents the corresponding time lag value when R_{ij} is the peak value.

3.6. Regression discontinuity design

We use Regression Discontinuity Design (RDD) to analyze the effect of a specific variable on the GNDVI degradation rate. RDD is widely applied to estimate the causal effect when a running variable crosses a particular threshold. The core principle involves utilizing an externally imposed “discontinuity” or “jump”, and by comparing samples near the threshold, RDD identifies causal relationships (Kemper et al., 2024). This method effectively simulates a natural experiment, overcoming potential selection bias and providing accurate estimates of causal effects. The model specification is as follows:

$$Y_i = \alpha_0 + \tau D_i + f(X_i - c) + \beta' Z_i + \varepsilon_i \quad (10)$$

where Y_i is the dependent variable and X_i is the independent variable. α_0 is the intercept, while τ represents the treatment effect at the threshold. c is the breakpoint (or threshold), which determines whether it is at the

demarcation point of the processing group. D_i is a binary indicator that equals 1 if $X_i > c$ and 0 otherwise. $f(X_i - c)$ is a smooth function of the running variable, typically specified as a polynomial or local linear form, with significance tests conducted during estimation. ε_i is the error term. Z_i represents a vector of covariates, and β' is the corresponding coefficient vector for the covariates. Including covariates helps to reduce bias from unobserved heterogeneity. The theoretical assumption is that the covariates are continuous at the threshold, implying they are unaffected by the crossing of the threshold.

3.7. Relative contribution decomposition method

This study employs a relative contribution decomposition method based on partial derivatives to quantify the influence of key driving factors on vegetation GNDVI dynamics of the QTP. The method combines the rate of change with partial derivatives, attributing GNDVI changes to specific variables. The study selects temperature, precipitation, potential evapotranspiration, and snow depth as the primary climate-related driving factors, with the remaining residual effects attributed to human activities. The model formula for any given raster cell are as follows:

$$C_m = \frac{\partial GNDVI}{\partial m} \times \frac{dm}{dt} \quad (11)$$

$$C_H = GNS - \sum_{m \in \{P, T, Pet, Sd\}} C_m \quad (12)$$

$$CR_m = \frac{|C_m|}{\sum_{m \in \{P, T, Pet, Sd\}} |C_m| + |C_H|} \quad (13)$$

$$CR_{CLM} = \sum_{m \in \{P, T, Pet, Sd\}} CR_m \quad (14)$$

$$CR_{HA} = 1 - CR_{CLM} \quad (15)$$

where, C_m represents the contribution of climate factor m to changes in GNDVI, while C_H denotes the contribution of human activities. The variable $m \in \{P, T, Pet, Sd\}$ corresponds to precipitation (P), temperature (T), potential evapotranspiration (Pet), and snow depth (Sd), respectively. GNS indicates the slope of change in GNDVI. CR_m is the relative contribution rate of climate factor m . CR_{CLM} represents the relative contribution rate of climate, and CR_{HA} represents the relative contribution rate of human activities.

4. Results

4.1. GNDVI change trend and transition type

Over the period 2000–2018, the vegetation cover of the QTP showed a generally improving trend, particularly around 2009, when the GNDVI changes exhibited significant spatial heterogeneity (Fig. 3). Detailed analysis reveals that during 2000–2009 and 2009–2018, the areas with improving vegetation (change rate >0.05%/a) accounted for 60.96% and 64.95% of the total area, respectively, with significant improvement areas (change rate >0.5 %/a) occupying 40.21% and 44.82%, respectively. From a spatial perspective, during 2000–2009, significant

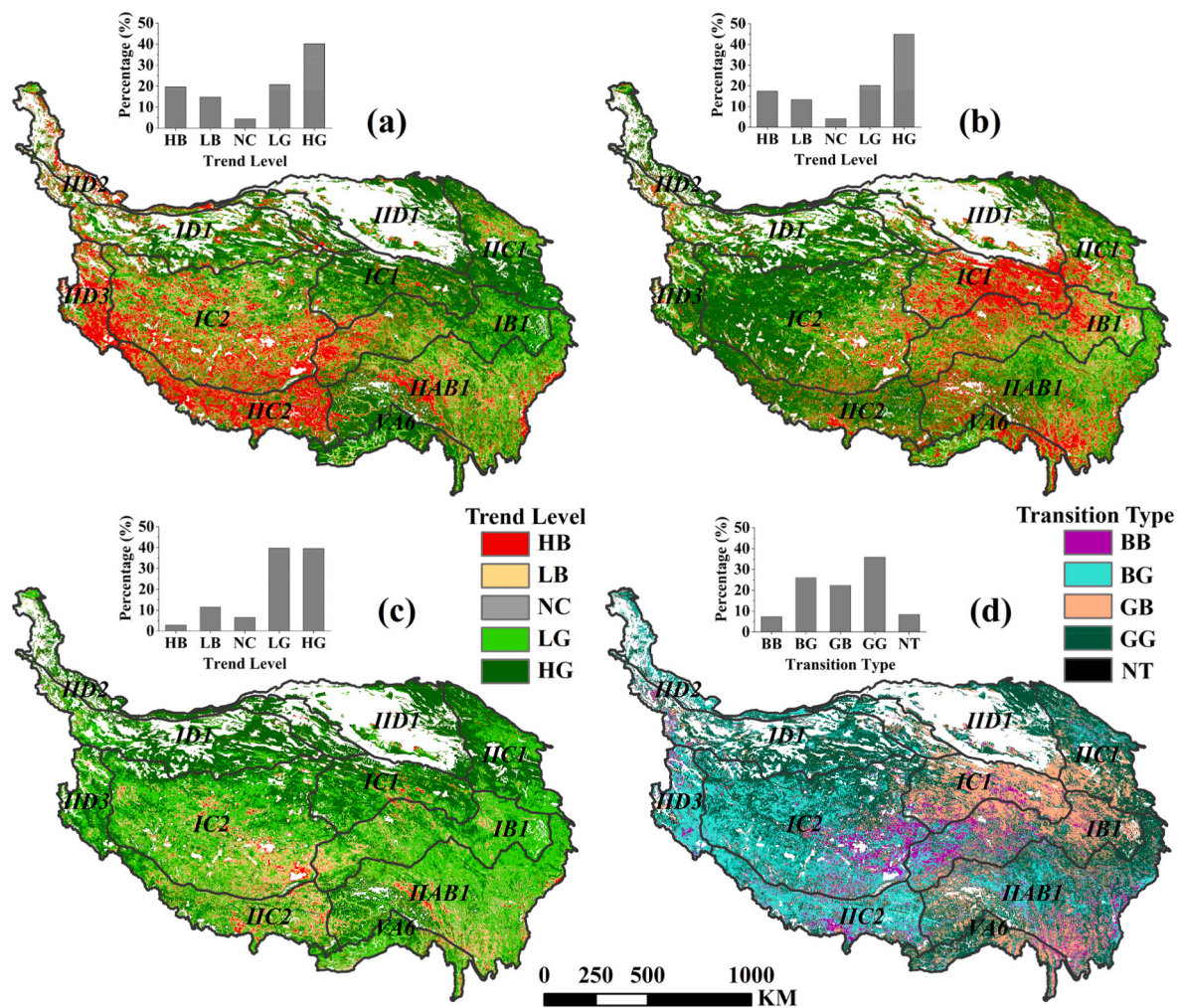


Fig. 3. GNDVI trend levels and transition types at pixel-scale: trend level during (a) 2000–2009, (b) 2009–2018, and (c) 2000–2018; (d) transition type from 2000 to 2018.

improvement in vegetation was mainly concentrated in the Sanjian-gyuan region in the northeast, while by 2009–2018, improvement areas shifted westward to the uninhabited regions, with a decrease in the extent of improvement in the southern forested areas. In terms of vegetation degradation, during 2000–2009, 34.48% of regions showed a degrading trend ($<-0.05\%/\text{a}$), of which 19.66% were significantly degraded ($<-0.5\%/\text{a}$); by 2009–2018, the proportion of degraded areas decreased by 3.68 %, and the proportion of significantly degraded areas correspondingly decreased by 1.47%. Spatially, the degraded areas were primarily concentrated in the southwest during the first decade, shifting to the southeast and central-eastern regions in the latter decade. Overall, during 2000–2018, 79.19% of the vegetation improved (with 39.52% showing significant improvement), while only 14.28% of the vegetation degraded (with a significant degradation rate of 2.78%). The significantly improved vegetation was mainly distributed in the northeast, while the significantly degraded vegetation was primarily found in areas with intense human activities, such as around roads and lakes/rivers.

Vegetation changes on the QTP showed significant variation. In the southwest, vegetation transitioned from browning to greening, while the northwest, northeast, and south experienced continuous greening. In central regions with concentrated human activities, vegetation showed continuous browning, or greening to browning. Statistics from vegetation change trends (Table 1) show that in the study area, significant improvement (39.55%) and continuous greening (35.87%) were dominant patterns. Among areas with significant improvement, continuous greening made up 21.81%, while in mildly improved areas, it accounted

for 12.88%. In degraded areas, transition patterns varied: significant degradation areas showed continuous browning (1.19%), whereas mildly degraded areas mainly experienced browning-greening (4.86%).

4.2. Natural driving factors of GNDVI trend

From 2000 to 2018, GNDVI on the QTP showed a clear vertical pattern: initial increase, then decrease, followed by another increase (Fig. 4a). Below 4500 m, vegetation improvement during 2000–2009 was generally higher than during 2009–2018, especially between 1500 and 3000 m. Notably, areas with significant GNDVI gains showed a tendency to migrate to higher altitudes, a phenomenon possibly related to the impact of global climate change on the plateau's ecosystem. As

Table 1

Proportion cross matrix of GNDVI change trend levels and transition types in Qinghai-Tibet Plateau from 2000 to 2018 (%).

Transition Types	Trend Levels					Total
	HB	LB	NC	LG	HG	
BB	1.19	2.94	0.84	1.91	0.43	7.31
BG	0.95	4.86	2.48	11.34	6.38	26.01
GB	0.45	2.26	1.46	9.19	9.02	22.38
GG	0.04	0.51	0.63	12.88	21.81	35.87
NT	0.15	0.95	1.03	4.39	1.91	8.43
Total	2.78	11.51	6.45	39.71	39.55	100.00

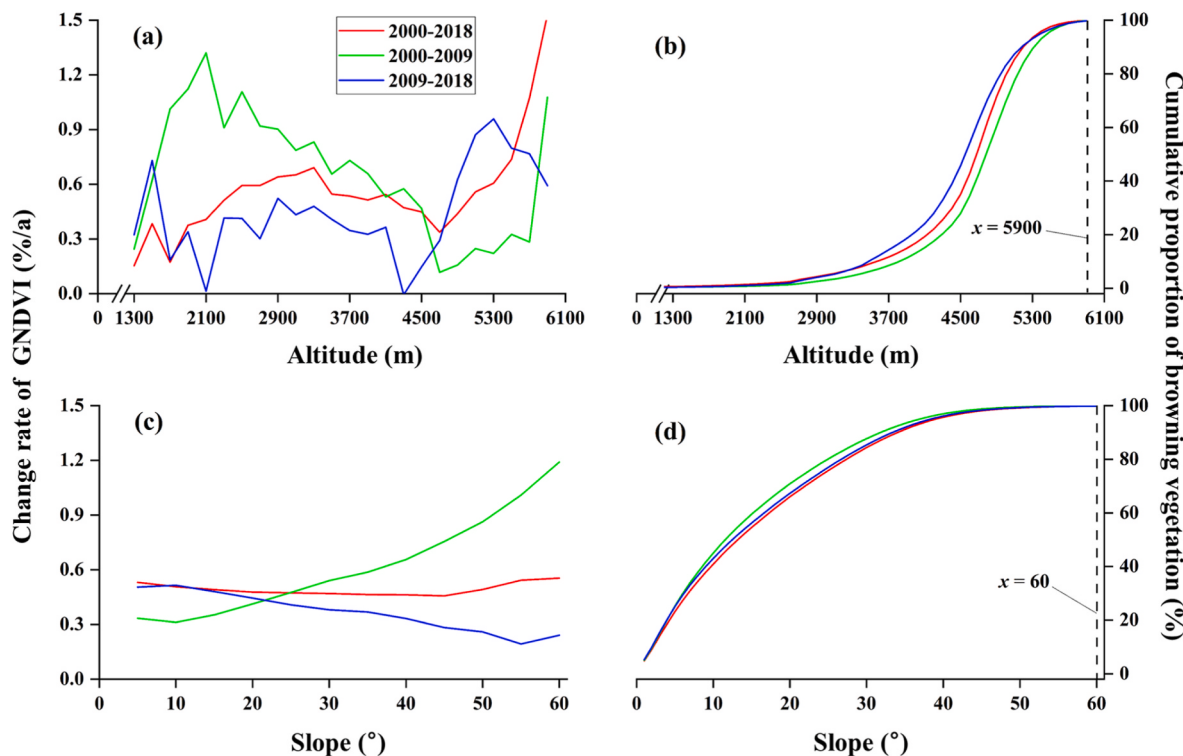


Fig. 4. Vegetation changes at different altitudes and slopes. (a) GNDVI change rate at different altitudes; (b) Cumulative proportion of browning vegetation at different altitudes; (c) GNDVI change rate on different slopes; (d) Cumulative proportion of browning vegetation on different slopes.

altitude increased, the proportion of browning vegetation areas exhibited a dynamic trend of first increasing and then decreasing. Spatially, browning vegetation was mainly concentrated between 4100 and 4900 m in the alpine zone (Fig. 4b). Compared to the first decade, browning vegetation increased in the 3300–4900 m range during the second decade.

In gentle slope areas ($<15^\circ$), GNDVI improvement showed a similar declining trend in both decades (Fig. 4c). In steep slope areas ($>25^\circ$), vegetation improvement during 2000–2009 was significantly higher than during 2009–2018. It showed an increasing trend, possibly due to more significant efforts of the Grain for Green and Grassland Programs in the first decade. Browning vegetation was mainly concentrated in gentle slope areas ($<15^\circ$) due to human activities such as grazing and farming. As the slope increased, the proportion of such degraded vegetation gradually decreased, and the area proportion of browning vegetation also diminished (Fig. 4d). During the second decade, vegetation degradation rebounded in steep slope areas, with the proportion of browning vegetation increasing compared to the first decade.

We analyzed the correlation between annual and growing season climate factors and GNDVI (Fig. 5). Histogram analysis shows that annual precipitation, growing season precipitation, annual average temperature, and growing season average temperature positively correlate with GNDVI. In contrast, annual potential evapotranspiration, growing season potential evapotranspiration, annual average snow depth, and growing season average snow depth negatively correlate with GNDVI. In terms of correlation strength, annual climate factors generally exhibit a stronger relationship than growing season with GNDVI, except for evapotranspiration. Overall, annual average temperature and precipitation are the most significant factors affecting GNDVI.

The influence of climatic factors on GNDVI exhibits clear elevation dependence. As elevation increases, particularly above 5000 m, the correlation between annual precipitation and GNDVI decreases significantly in most eco-geographical regions (Fig. 6a). This phenomenon may be partly due to lower temperatures at higher altitudes, which

offset the positive effect of precipitation on vegetation growth. In contrast, the correlation between annual mean temperature and GNDVI typically increases with elevation in areas below 4000 m, suggesting that the rise in temperature has a positive impact on vegetation growth (Fig. 6b). Notably, a negative correlation between temperature and GNDVI is observed in the low-elevation areas of VA6. This could be because these temperate regions have already reached the optimal temperature threshold for vegetation growth at lower elevations, and further increases in temperature may exacerbate water stress, thus inhibiting vegetation growth. The correlation between evapotranspiration and GNDVI follows a more complex pattern, generally strengthening with increasing elevation. However, in regions such as VA6, IIC1, and IIC2, there is an inflection point, with different trends emerging on either side of the 4000–5000 m elevation range (Fig. 6c). Regarding snow depth, below 5000 m, there is generally a negative correlation with GNDVI, which strengthens as elevation increases (Fig. 6d).

In QTP, vegetation in arid and semi-arid regions is more sensitive to water restriction, resulting in a higher correlation between precipitation and GNDVI than in humid areas. Unlike in humid areas, the temperature rise in arid and semi-arid areas, such as the decrease of soil moisture and the increase of evapotranspiration, is more obvious, leading to more serious water stress. In sub-frigid zone, the correlation between temperature and GNDVI is usually higher than that in temperate zone (such as IC1>IIC1, ID1>IID1), and the correlations in these zones are generally higher than that in tropical zone. Potential evapotranspiration has a strong correlation with GNDVI in temperate and tropical regions, while snow depth shows the strongest negative correlation in cold and dry areas (such as ID1).

4.3. Human driving factors of GNDVI trend

From 2000 to 2018, as the distance to roads increased, vegetation GNDVI change on the QTP showed a significant upward trend (Fig. 7a). Research shows that vegetation improvement in road buffer zones was overall higher during 2000–2009 than 2009–2018. Notably, regions

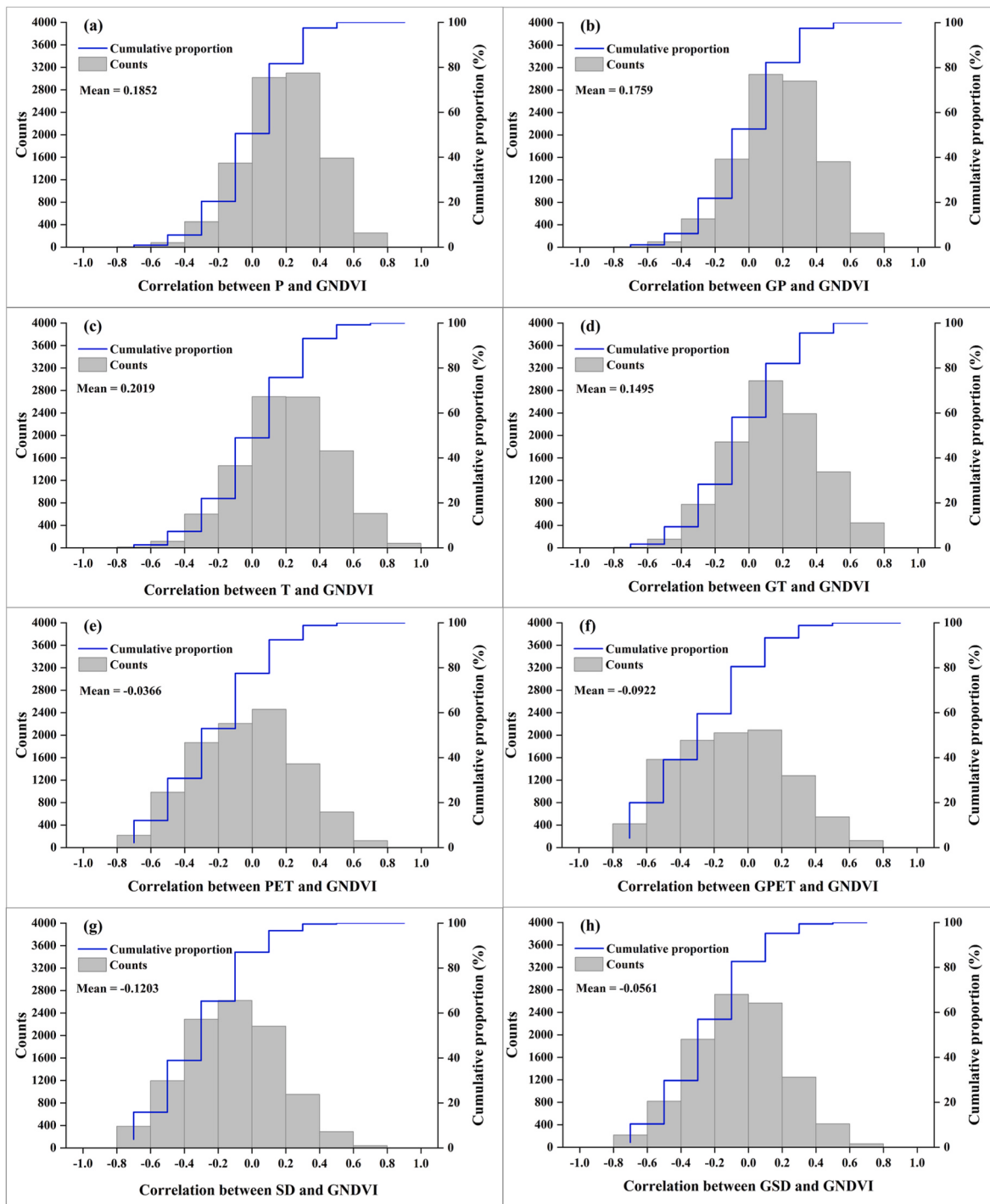


Fig. 5. Distribution histogram of correlation between climate factors and GNDVI. **(a)** Annual precipitation and GNDVI. **(b)** Growing season precipitation and GNDVI. **(c)** Annual average temperature and GNDVI. **(d)** Growing season average temperature and GNDVI. **(e)** Annual potential evapotranspiration and GNDVI. **(f)** Growing season potential evapotranspiration and GNDVI. **(g)** Annual average snow depth and GNDVI. **(h)** Growing season average snow depth and GNDVI.

with larger GNDVI increases exhibited a trend of away from roads. Meanwhile, browning vegetation proportion decreased with distance from roads, with over 70 % concentrated within 10 km. This may be related to roads facilitating human activities such as grazing, transportation, and tourism. Additionally, browning vegetation showed a slow expansion towards areas farther from roads in the second decade compared to the first (Fig. 7b).

Research indicates that with increasing distance from rivers/lakes, the GNDVI change rate from 2000 to 2018 shows moderate fluctuations, but significant differences are observed between the two decades

(Fig. 7c). Within a 25 km buffer zone around rivers/lakes, vegetation improvement was stronger during 2000–2009 compared to 2009–2018. Beyond 25 km, this trend reverses, and the rate of change exhibits an opposite trend as the distance increases. This spatial variation likely relates to human activities, such as grazing and tourism, concentrated near rivers/lakes, with approximately 40% of browning vegetation concentrated within 10 km of rivers (Fig. 7d). Notably, browning vegetation is highly clustered near rivers/lakes, gradually spreading towards adjacent areas.

From 2000 to 2018, there was a significant correlation between

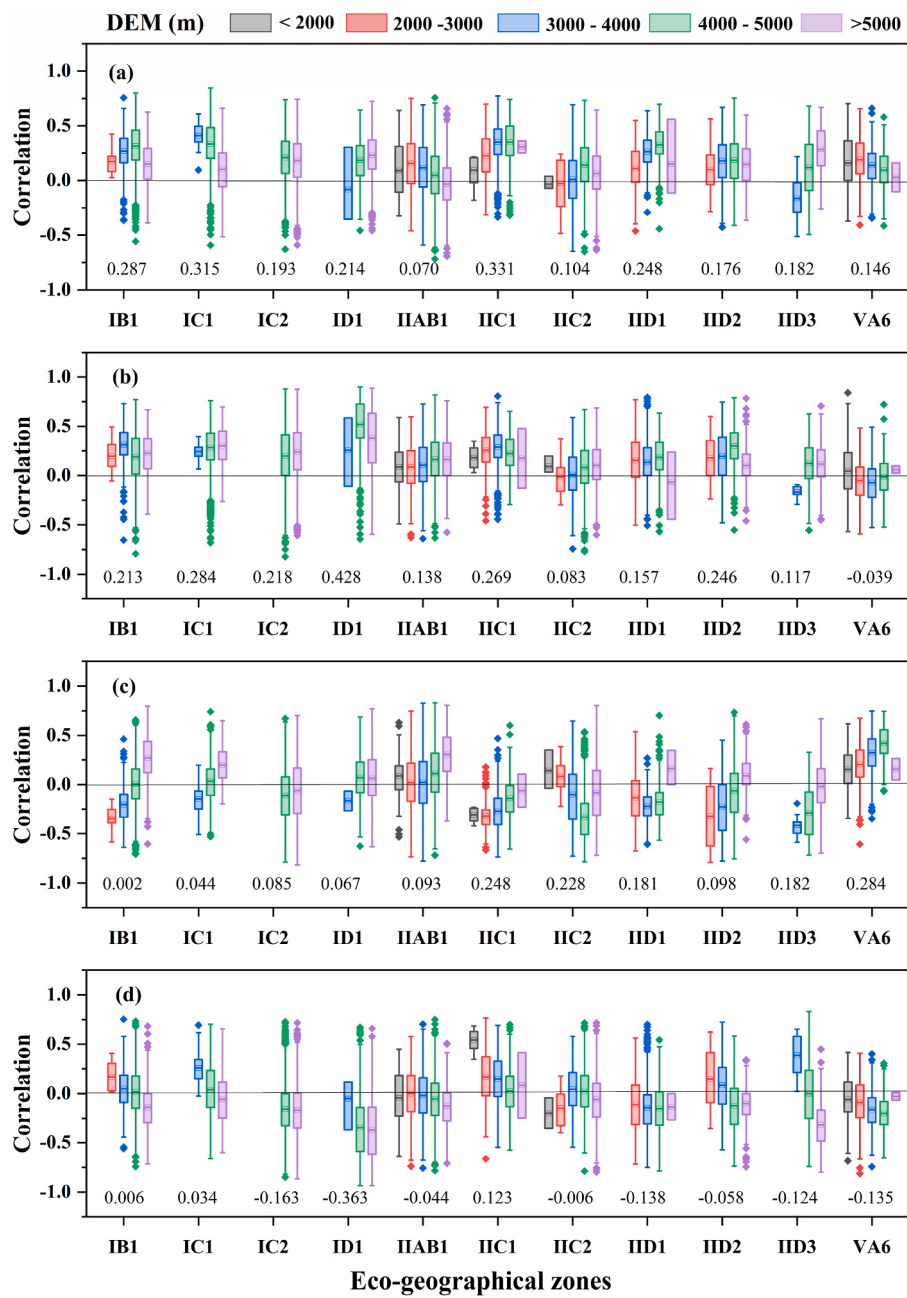


Fig. 6. Vertical distribution of the correlation between climate factors and GNDVI in different eco-geographical regions. **(a)** Annual precipitation and GNDVI. **(b)** Annual average temperature and GNDVI. **(c)** Annual potential evapotranspiration and GNDVI. **(d)** Annual snow depth and GNDVI.

changes in the GNDVI and population density across the QTP (Fig. 8a). Overall, in eco-geographical regions with lower population densities—such as IC1, IID1, and IID2—the rate of change in GNDVI was generally positive and relatively high. In contrast, in regions with higher population densities, particularly in IIC2 and IIAB1, the GNDVI change rate may be negative, potentially indicating a higher proportion of vegetation degradation. When population density was below 20 pop/km², the GNDVI change rate was generally negatively correlated with population density. However, once this threshold was exceeded, the relationship often shifted, suggesting more complex interaction mechanisms. Notably, in the IIC1 region, where population density was also below 20 pop/km², an increasing population density was associated with a more pronounced greening trend in GNDVI. This pattern deviates markedly from those observed in other regions and may reflect unique local human–environment relationships or specific management

policies. In terms of vegetation types, GNDVI change rates for forests, scrubs, and meadows were relatively similar and showed only minor fluctuations. In contrast, steppes exhibited a greater range of GNDVI change rates and a more dispersed distribution, which may reflect the higher sensitivity of grassland ecosystems to external disturbances such as grazing. As an important indicator of human activity, grazing intensity likely played a substantial role in influencing GNDVI dynamics in the QTP. From 2000 to 2018, the total livestock population in Qinghai and Tibet showed an overall declining trend, though notable differences were observed across different time periods (Fig. 8b). In Qinghai, livestock numbers slightly decreased between 2000 and 2009, then rose modestly from 2009 to 2018, which corresponds to a transition in GNDVI trends from greening to browning. In contrast, livestock numbers in Tibet initially increased and then declined, aligning with a shift in local GNDVI trends from browning to greening.

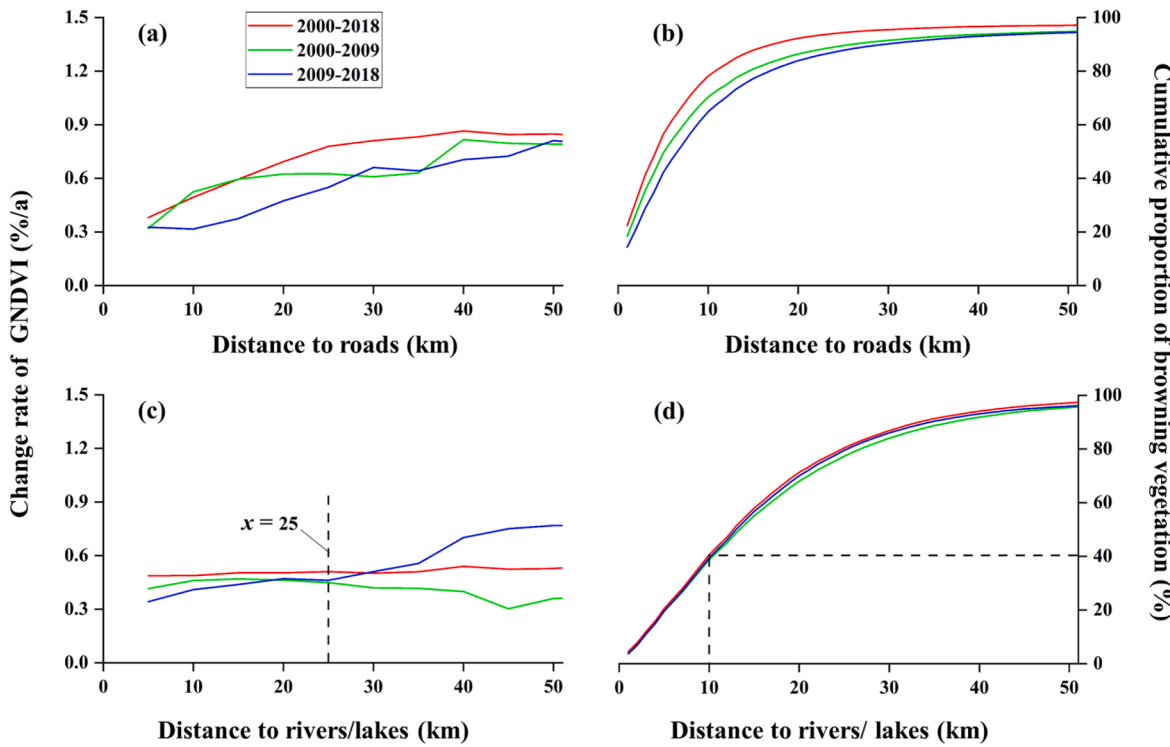


Fig. 7. Impact of distance to roads and rivers/lakes on vegetation Changes. (a) Relationship between distance to roads and change rate in GNDVI. (b) Relationship between distance to roads and cumulative proportion of browning vegetation. (c) Relationship between distance to rivers/lakes and changes in GNDVI. (d) Relationship between distance to rivers/lakes and cumulative proportion of browning vegetation.

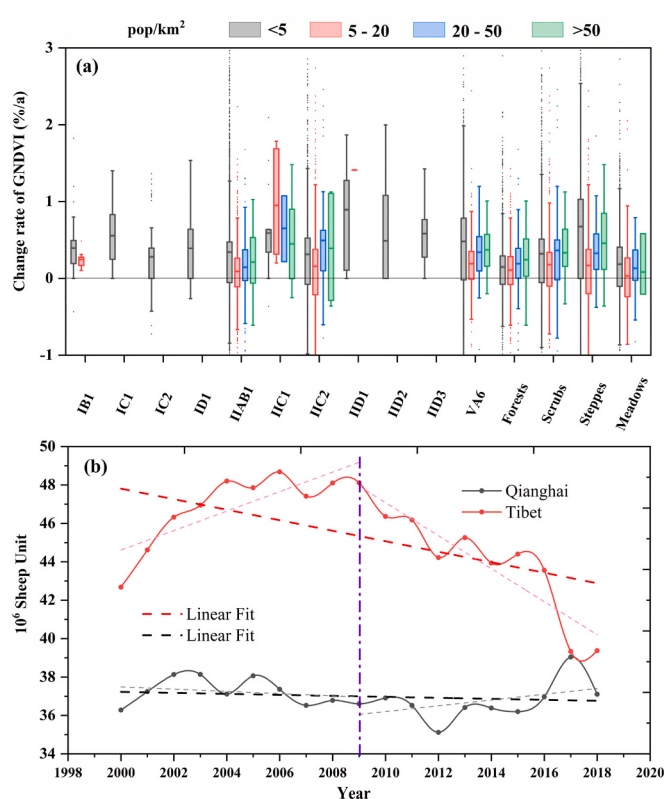


Fig. 8. Population density and grazing patterns analysis in QTP. (a) Variation characteristics of GNDVI with population density in different eco-geographical regions and vegetation types. (b) Livestock quantity changes in Qinghai and Tibet from 2000 to 2018.

4.4. Time lag effect and threshold effect

The lag correlation between climate factors and GNDVI indicates that a small part of regions experience a lag effect of 1–4 months (Fig. 9). Among these factors, the lag effect of temperature, precipitation, and snow depth is confined to region area less than 40,000 km², with a predominant 4-month lag. In contrast, the lag effect of potential evapotranspiration is more evenly distributed across the 1–4 month range, but overall, it shows a much broader lag effect area, reaching 95,644 km². In terms of the spatial patterns associated with GNDVI, the lag effect of precipitation is mainly observed in the eastern part of the QTP, particularly in regions such as IIC1 and IB1. The lag effect of temperature is primarily found in the central, northwestern, and eastern parts of the QTP. The lag effect of potential evapotranspiration is most prominent in the southern part of the QTP, including regions like IC2, IID3, and IIC2, while the lag effect of snow depth is mainly seen in the northwestern part of the plateau.

We conducted RDD to examine the threshold effects influencing vegetation degradation (Fig. 10). The results indicate that the impact of population density on the GNDVI change rate is significant, with no systematic differences in covariates on either side of the breakpoint. Overall, as population density increases, the GNDVI change rate shows a downward trend. However, when population density exceeds 17 pop/km², the fitted line becomes flatter, indicating that beyond this threshold, the effect of population density on the GNDVI change rate may reach marginal effect (Fig. 10a). Robustness checks reveal that, across different bandwidths, the breakpoint regression coefficients consistently show negative effects, though there are significant differences in statistical significance and effect size. Overall, the regression coefficients demonstrate the trend that “the effect strengthens as bandwidth decreases,” with the core results remaining robust within a bandwidth range of 0.5–1.25 times. Similarly, grazing intensity significantly affects the GNDVI change rate. As grazing intensity increases, the

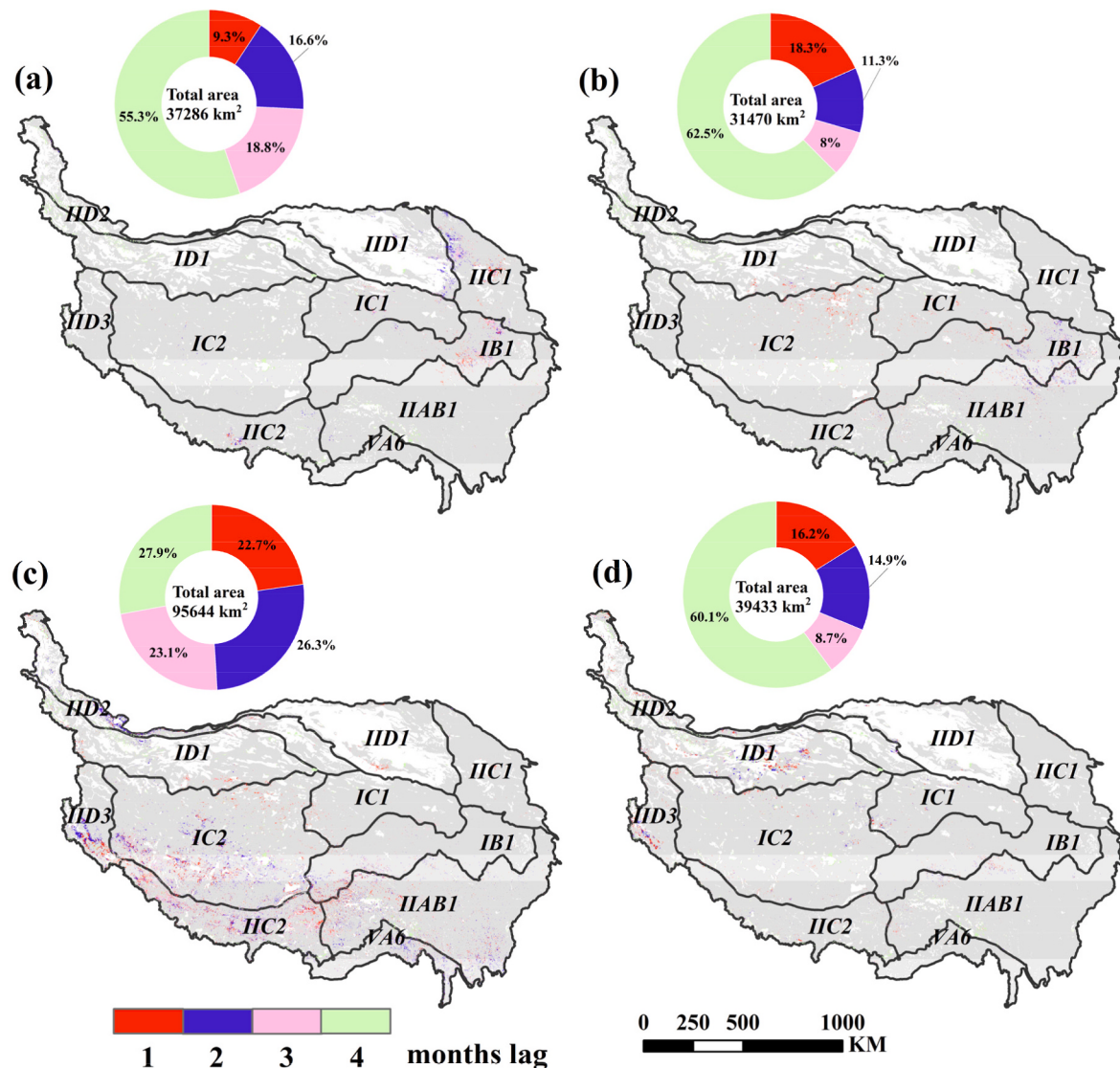


Fig. 9. Time lag correlation between climate factors and GNDVI. (a) Precipitation. (b) Temperature. (c) Potential evapotranspiration. (d) Snow depth.

GNDVI change rate decreases. The critical threshold is 250 SU/km², beyond which the decline of change rate in GNDVI becomes more pronounced (Fig. 10b). Robustness checks show that the breakpoint regression coefficients exhibit positive effects, and the core results remain robust within a bandwidth range of 0.25–1.50 times.

4.5. Contribution rate of driving factors to GNDVI

We quantified the contribution rate of climate factors and human activities to the changes in GNDVI across different eco-geographical regions (Fig. 11). Precipitation typically accounts for 25%–50% of GNDVI variation, while temperature generally contributes less than 5%. In contrast, the contribution rate of potential evapotranspiration is more dispersed, but it plays a more significant role in the southern regions of the QTP. Snow depth contributes relatively little to GNDVI variation, typically less than 5%. Overall, climate factors contribute more than 50% to GNDVI changes. In comparison, human activities generally account for more than 30%, although in some areas of the central and southern QTP, the contribution is lower than 30%, with some regions even below 15%.

On average, precipitation contributes significantly more than other climate factors across all ecological regions, and together with human activities and, together with human activities, predominantly drives

GNDVI changes, highlighting the importance of these two factors. In various eco-geographical regions, temperature has a larger contribution to GNDVI changes in the colder ID1, IC2, and IC3 zones (Fig. 11g). The greatest contribution of evapotranspiration occurred in the hot and humid VA6 region, while snow depth exerts a greater influence on GNDVI changes occurred in the temperate arid IID3 region. Regions with significant differences between the contributions of climate factors and human activities are mainly concentrated in the temperate semi-arid zones IIC1 and IIC2.

5. Discussion

5.1. Comparison with previous studies

This study monitors the overall greening and ecological restoration trends of vegetation on the QTP, emphasizing the synergistic role of climate change and human activities in driving vegetation dynamics. The findings align with several previous studies. For example, Sun et al. (2023) found that the warming and wetting trends extended the growing season and accelerated plant green-up, thereby significantly enhancing vegetation indices. This result is consistent with our observation of a positive correlation between precipitation, temperature, and GNDVI (Fig. 5). However, this correlation is not spatially uniform; some areas

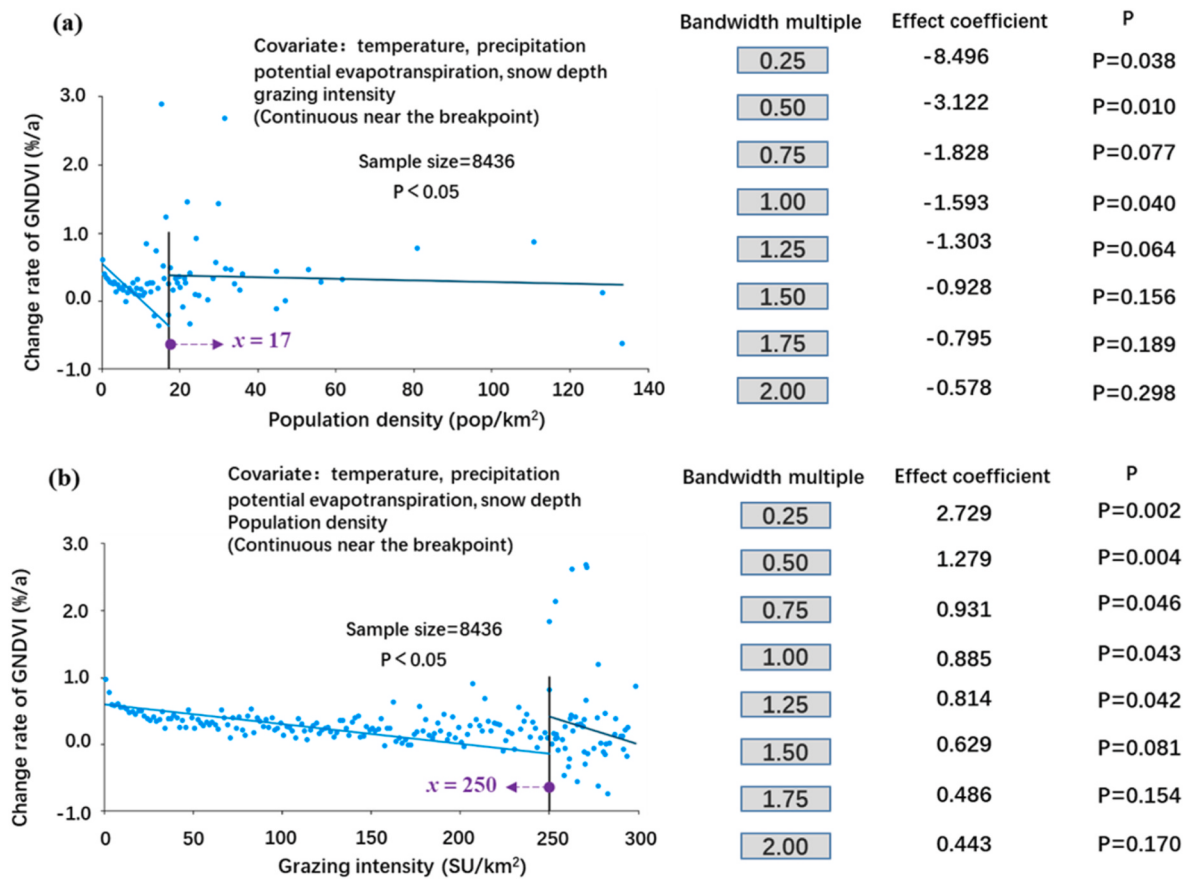


Fig. 10. Threshold effect analysis. (a) Population density affects the change rate of GNDVI. (b) Grazing intensity affects the change rate of GNDVI.

exhibit a negative correlation between precipitation, temperature, and GNDVI, suggesting that once temperature or precipitation exceeds certain ecological thresholds, sustained warming and wetting may suppress vegetation growth. Lu et al. (2024) further pointed out that extreme precipitation events could adversely affect vegetation growth on the QTP, while the spatiotemporal uniformity of precipitation might be more beneficial to vegetation growth. Our study also supports this view, showing that on an annual scale, the correlation between precipitation, temperature, and GNDVI is significantly stronger than on the growing season scale (Fig. 5). Furthermore, the rate of change in climate factors may be more ecologically significant than their total amounts and may be accompanied by lag effects (Lu et al., 2023b). Therefore, the temporal structure of precipitation could have profound impacts on vegetation dynamics (Fig. 9), especially in the plateau regions. The temporal structure of precipitation may play an important role in regulating vegetation dynamics, particularly in QTP, as the unique land-sea thermal differences and monsoon systems may also regulate regional hydrological processes by influencing precipitation variability (Lu et al., 2023a).

We found that the elevation gradient significantly modulates the strength of the temperature's effect on vegetation growth, with the correlation between GNDVI and temperature significantly increasing with altitude (Fig. 6). In the context of climate warming, this mechanism becomes more pronounced, manifesting as the migration of high GNDVI values to higher altitudes. This phenomenon is also supported by Wei et al. (2022), whose study indicates that vegetation conditions in high-altitude regions are continuously improving. Zhou et al. (2025) noted that among various climate factors, the impact of precipitation might be more direct. Our contribution rate analysis also confirms this, indicating that precipitation is the primary climate factor influencing GNDVI (Fig. 11). Regarding human activity impacts, we identified the

grazing intensity threshold leading to extreme vegetation degradation as 250 SU/km² (Fig. 10). This threshold may be high, as 95% of the study area has grazing intensities lower than this value. However, Zhu et al. (2023) pointed out that only 80% of the QTP has grazing intensity below the extreme threshold. We speculate that this discrepancy may stem from scale effects caused by differences in data resolution.

5.2. Heterogeneity and elevational dependence of climatic impacts on GNDVI

Climatic impacts on vegetation growth varied spatially, with regional and altitudinal differences (Figs. 6 and 11). As research shows (Yang et al., 2022; Jia et al., 2024), water conditions were confirmed to be the primary limiting factor for vegetation growth in temperate ecosystems, with the stress effect intensifying with increasing aridity. Based on the rainfall limitation theory, insufficient spring and winter precipitation on the QTP led to bud and leaf desiccation in some vegetation, thereby restricting vegetation growth. This mechanism was particularly pronounced in the arid-semi-arid regions of the southwest and northeast of the plateau, where precipitation became the dominant climatic factor for vegetation growth (Fig. 12).

From 2000 to 2009, reduced precipitation in the QTP's southwest caused vegetation browning in that region. Notably, the degree of vegetation degradation in the arid zone (IID3) was significantly higher than in the semi-arid zone (IIC2), reflecting the regulatory role of the aridity gradient on vegetation responses (Fig. 3). With increasing altitude, water stress diminished, and low-temperature stress emerged as the main factor affecting vegetation growth. Therefore, under the same conditions of reduced precipitation, the degree of vegetation degradation in the southern sub-frigid zone IC2 was significantly lower than in the semi-arid IIC2 zone, while the northern IC2 zone even showed a

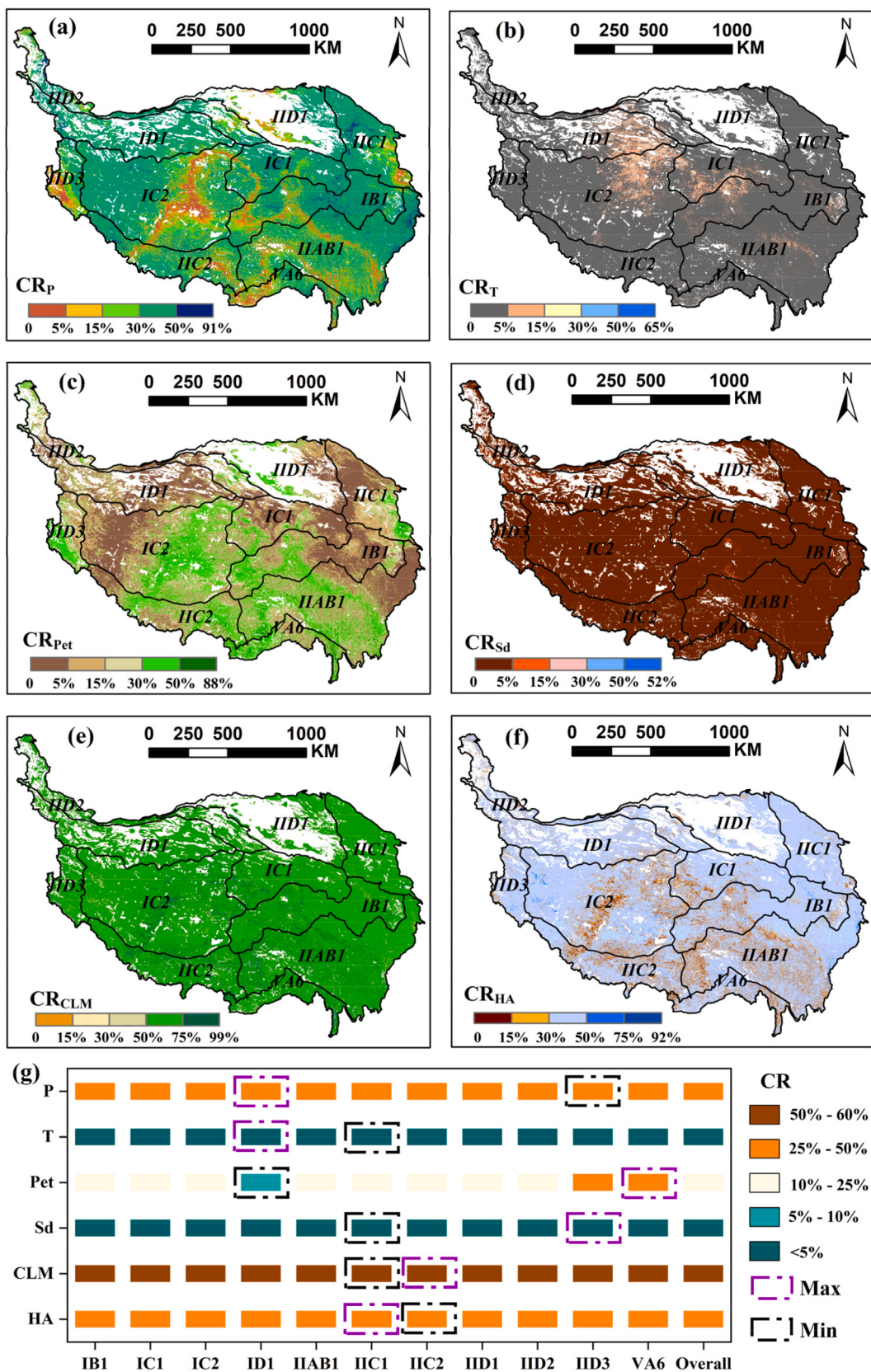


Fig. 11. Analysis of contribution rate of factors to GNDVI change. **(a)** Contribution rate of precipitation. **(b)** Contribution rate of temperature. **(c)** Contribution rate of potential evapotranspiration. **(d)** Contribution rate of snow depth. **(e)** Contribution rate of climate. **(f)** Contribution rate of human activities. **(g)** Contribution rate of each factor affecting the change of GNDVI in eco-geographical region.

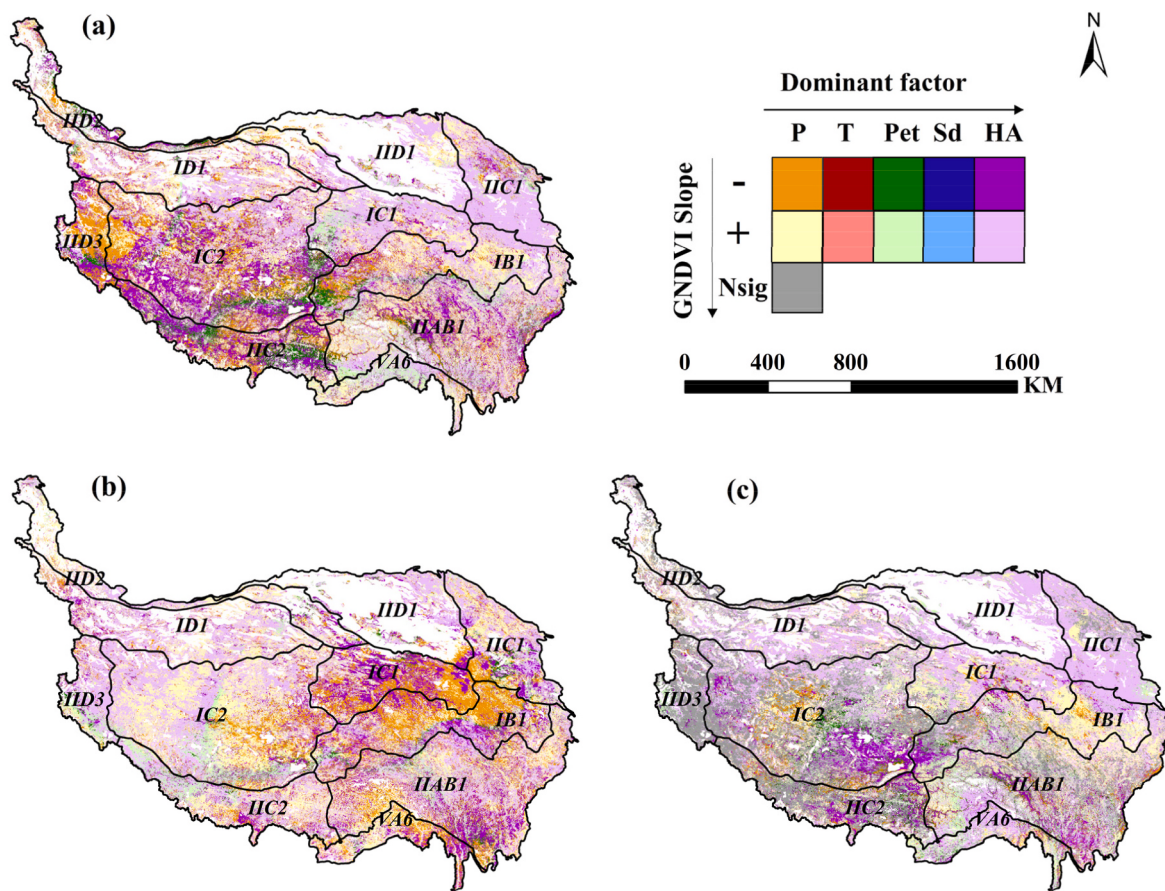


Fig. 12. Temporal and spatial distribution of dominant factors of vegetation GNDVI change in Qinghai-Tibet Plateau. (a) 2000–2009. (b) 2009–2018. (c) 2000–2018. The slope of GNDVI has positive and negative trends, and the dominant factors are precipitation, temperature, potential evapotranspiration, snow depth and human activities.

greening trend due to increased temperatures. During 2009–2018, the reduced precipitation pattern shifted, moving the vegetation browning center from the southwest to the northeast of QTP. This period's observations confirmed the strong link between aridity and vegetation degradation, with IC1's semi-arid degradation far exceeding that in the semi-humid IB1 zone. This shift reflects both the spatial heterogeneity of regional climate change and the complexity of ecosystems' responses to it. Additionally, the study indicated that the vegetation change process did not occur synchronously with climate change, further revealing the lag in ecosystem responses to climate change.

5.3. Offset effects of human activities on the climatic impacts on GNDVI

Since its initiation in 1999, China's Grain for Green (GFG) Program has primarily targeted farmland with slopes greater than 25°, aiming to improve vegetation cover and significantly enhance the ecological environment in various regions (Peng et al., 2014; Liu et al., 2022). Research indicates that ecological restoration projects have played a crucial role in vegetation recovery across China (Song et al., 2022). In certain areas of the QTP, especially in regions with higher population densities, the GFG policy has had a significant positive impact on vegetation growth (Fig. 13). However, the implementation of this program has followed a phased approach. Compared to the 2000–2009 period, the intensity of the program's implementation in the QTP significantly weakened during the 2009–2018 period (Guo et al., 2023). Although a warming and moistening trend in the steep areas of the QTP between 2009 and 2018 was conducive to vegetation growth, the reduced intensity of the GFG program partially offset these climatic benefits. Consequently, the GNDVI growth rate in steep areas during this

period declined significantly, and vegetation browning spread to even steeper regions (Fig. 4). These changes reflect the complex interactions between ecological projects and climate change. While climate change provides some potential for ecosystem restoration, this potential has not been fully realized due to weakened human intervention, particularly the reduced intensity of ecological restoration projects. Therefore, under the context of climate change, the implementation intensity and pace of ecological restoration policies should be dynamically adjusted based on regional characteristics to maximize their restoration effectiveness. Relying solely on improved climatic conditions is insufficient for achieving long-term ecological stability; targeted human interventions are also necessary to enhance ecosystem adaptability and recovery capacity in the face of external disturbances.

Despite the low overall population density in the QTP, its inherent high vulnerability amplifies its impact. Under similar natural conditions, population density exhibits a significant positive correlation with human activity intensity (Ehrlich et al., 2018). Rising population density usually intensifies activities like grazing, agriculture, tourism, and transportation, increasing environmental pressure (Mu et al., 2022). Increasing population density can negate some climate change benefits for vegetation while worsening its adverse effects (Li et al., 2017; Wellmann et al., 2020). This mechanism is confirmed across different ecological and geographical regions of the QTP: despite warming and moistening trends, GNDVI change rates decline significantly with rising population density. In fragile areas, human activities offset climate benefits more strongly, with GNDVI trends linked to population density being more pronounced in arid and semi-arid regions than in humid ones (Fig. 8). Further analysis indicates that compared to the 2000–2009 period, during 2009–2018, the population density in regions distant

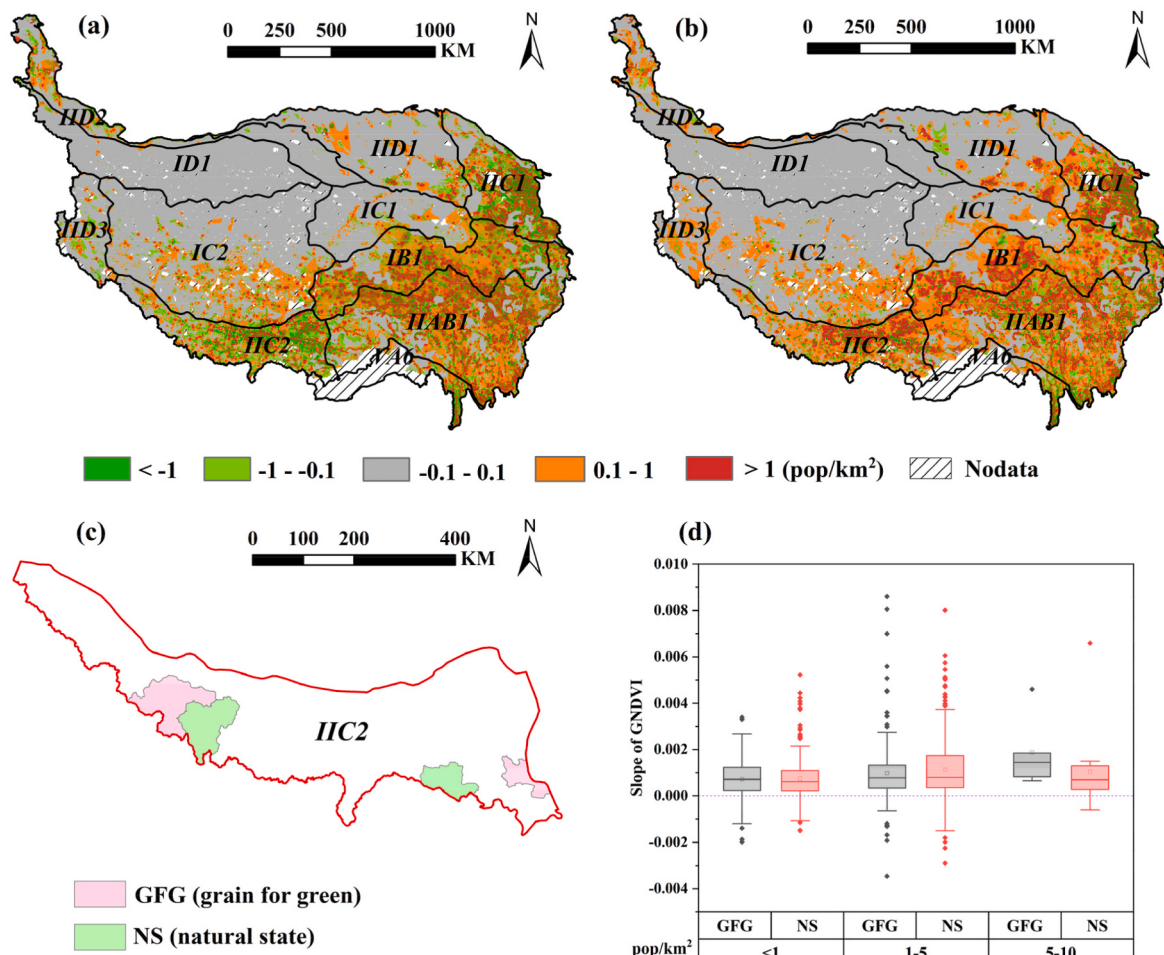


Fig. 13. Population density changes in Qinghai-Tibet Plateau and effect of GFG (grain for green). (a) Population density changes in 2000–2009. (b) Population density changes in 2009–2018. (c) Implementation of GFG (grain for green) in IIC2. (d) Comparison of GNDVI slope.

from high GNDVI areas grew at an accelerated rate, leading to a significant intensification of vegetation browning (Fig. 13). This suggests that in certain regions and periods, human activities' negative effects on vegetation may have outweighed climate change benefits. Therefore, ecological protection and management strategies must place greater emphasis on the interplay between human activities and climate change, advocating for better methods to harmonize their relationship, especially in ecologically fragile regions.

Grazing, particularly overgrazing, and tourism activities have been shown to lead to a significant decline in vegetation greenness (Fig. 10), with these activities primarily concentrated around roads and lakeside areas. Consequently, vegetation browning near roads and lakes on the QTP is consistent across periods, with more severe browning in central and southwestern regions, aligning with prior studies (Zhu et al., 2023). As the distance to roads and lakes increases, the offset effects of human interventions diminish, resulting in a significant rise in the GNDVI change rate of vegetation. It was found that regardless of other factors, grazing intensity was obviously negatively correlated with the change rate of GNDVI, and the vegetation condition deteriorated significantly after exceeding a certain threshold (Fig. 10b). This indicates that intensified grazing amplifies climate change's negative effects on vegetation, especially in areas with high human activity (Zhang et al., 2018). Existing studies point out that the livestock population in the northeastern part of the QTP has been steadily increasing (Wang et al., 2024), partially offsetting warming and moistening benefits for vegetation, reducing GNDVI change rates. In contrast, despite fragile conditions and slight precipitation decline in sparsely populated

northwestern regions, GNDVI increases due to conservation efforts like national nature reserves (Li et al., 2020). This comparison shows that well-designed conservation projects can counteract climate change's negative effects on vegetation, fostering recovery and improvement.

5.4. Policy implications

Climate change, human activities, and species traits collectively drive significant vegetation shifts, posing major threats to ecosystems. Studies indicate that 2000–2009 ecological projects, like farmland-to-forest conversions, promoted vegetation recovery, especially in steep and grassland areas. However, as policy enforcement weakened over time, the vegetation recovery effects in some regions failed to be sustained, intensifying browning. This suggests that singular ecological protection measures, lacking long-term and stable support, face the risk of ecological rebound. The impact of climatic factors on vegetation exhibits an explicit altitudinal dependency: low-altitude regions are primarily influenced by changes in precipitation, while high-altitude regions are constrained by temperature variations. Ongoing global warming will result in high-frequency community reorganization and replacement (Zhang et al., 2017a). Simultaneously, human activities (such as overgrazing and tourism development) further exacerbate vegetation degradation pressures in high-altitude and vulnerable ecological zones.

Based on the results of this study, several policy measures are recommended. First, the establishment of a stable and long-term ecological investment mechanism is crucial, particularly in areas where vegetation

degradation is severe, such as the densely populated, relatively low-slope regions in the southeast and central-east parts of QTP. To prevent ecological rebound or secondary degradation caused by interruptions in funding or policy, it is essential to ensure the sustainability and continuity of funding for restoration projects. In high-altitude and steep-slope areas, it is necessary to strengthen the development of a continuous monitoring system. This should integrate multi-source remote sensing monitoring with ground-based sampling points, forming a comprehensive technical system to scientifically evaluate the long-term effects of ecological restoration projects, and dynamically adjust policies based on the results of these assessments (Cavender-Bares et al., 2022). Second, a region-specific management strategy should be implemented. Given the spatial unevenness of the coupling between climate stress and human activities, it is important to develop management strategies tailored to specific areas. In low-altitude regions, attention should be focused on the rational allocation of water resources during the rainy season and the enhancement of soil conservation capabilities. In areas with slopes less than 15° and near water bodies or roads, promoting water-conserving vegetation and drought-resistant native grass species, along with crop rotation and the establishment of ecological buffer zones, should be prioritized to reduce human interference intensity (Liu et al., 2022). In high-altitude regions, climate-adaptive management should be given priority, specifically including vegetation optimization based on temperature gradients, adjustments to land use structures, and reforestation strategies involving cold-tolerant herbaceous plants and shrubs. Third, stricter supervision of human activities and ecological risk control are needed. Within the legal framework of the "Law of the People's Republic of China on Ecological Protection in the Qinghai-Tibet Plateau" (PRC, 2023), efforts should be made to promote the establishment of an ecological space governance system centered around a network of protected areas. In the southeast and southwest, where overgrazing and tourism activities are significant, pilot projects should be launched to implement a "carrying capacity assessment + use restrictions + digital monitoring" coordination mechanism. This mechanism would include dynamic grazing limits and rotational grazing systems through the installation of digital fences and drone patrols in high-density grazing areas (Augustine et al., 2020). For regions where grazing intensity exceeds 250 SU/km², an "ecological red line" should be established, mandating grazing restrictions or migration policies, thereby reducing the sustained pressure on vegetation and preventing irreversible grassland degradation. Finally, a comprehensive ecological compensation system (Dobšinská et al., 2024) should be established to facilitate a positive interaction between conservation and development. In regions significantly affected by both climate and human pressures, such as IIC1 and IIC2 zones, it is recommended to establish a compensation mechanism based on dynamic GNDVI indicators. At the same time, the development of green industries such as low-carbon pastoralism, origin-based organic agricultural products, and community-based eco-tourism should be promoted to achieve coordinated economic and ecological development. By implementing these measures, a more comprehensive framework for vegetation protection will be established, enhancing regional ecological security and promoting continuous improvements in the ecological environment.

5.5. Limitations and future research

This study has limitations in data selection. Firstly, sensor replacement or aging has led to inconsistent conclusions regarding NDVI changes across different data sources for the QTP. For example, during the 2000–2012 period, studies using GIMMS3g data showed a decline in QTP GNDVI, while SPOT and MODIS studies found opposite trends (Shen et al., 2015; Pang et al., 2017). Secondly, MODIS C6 data, compared to earlier versions, has improved quality by correcting errors and optimizing algorithms. However, without long-term field data, satellite NDVI may underestimate alpine vegetation growth trends (Wang et al., 2021). Future research can overcome these limitations by

enhancing the validation of ground observation data, conducting multi-source data fusion analyses, and incorporating advanced techniques such as machine learning.

This study has limitations in analyzing the vegetation changes and their driving mechanisms on the QTP. First, the research primarily focuses on the impact of precipitation, temperature, potential evapotranspiration, and snow depth on vegetation, while neglecting other key factors such as solar radiation, CO₂ levels, and atmospheric circulation. Previous studies have shown that these factors may interact through complex system feedbacks to influence vegetation growth (Piao et al., 2012; Li et al., 2023; Zhang et al., 2023). Second, the study lacks process-based modeling, which limits a deeper understanding of the driving mechanisms. Moreover, it does not systematically reveal the coupled driving mechanisms of natural and human-induced factors from a multi-scale perspective, nor incorporate future vegetation change predictions into the ecosystem management decision-making framework. Therefore, future research could integrate the LPJ-GUESS model and scenario simulations (Kocev et al., 2009; Bagnara et al., 2019; Fathollahi et al., 2024) to expand multi-factor analysis and multi-scale simulations, uncover system feedback mechanisms, and link them with ecosystem management to support regional ecological protection and sustainability.

6. Conclusions

This study systematically investigated the temporal trends and driving mechanisms of GNDVI across the QTP from 2000 to 2018, with a particular focus on the impacts of climate change and human activities on vegetation dynamics. The results indicate an overall greening trend in vegetation across the QTP, although localized browning was observed. Vegetation growth was influenced by both natural and anthropogenic factors, exhibiting significant spatiotemporal heterogeneity and elevation dependency. Some climatic variables showed lagged effects in local regions, whereas the influence of human activities displayed a threshold effect. Precipitation and human activities were identified as the dominant drivers of GNDVI variations. Specifically, precipitation contributed approximately 25%–50% to GNDVI changes, while the contribution from human activities often exceeded 30%, though their spatial impacts varied considerably. In arid and semi-arid areas, precipitation is the main driving factor for the change of GNDVI, while in humid or cold areas, the contribution of temperature is also great. With increasing elevation, the influence of precipitation on GNDVI weakened, while the effect of temperature became more pronounced. Human activities—particularly grazing and tourism near roads and lakes—exerted significant negative impacts on GNDVI, partially offsetting the positive effects of warming and increased moisture. Furthermore, when population density exceeded 17 pop/km², its influence on the GNDVI rate of change approached a marginal effect; when grazing intensity surpassed 250 SU/km², its negative impact on GNDVI intensified markedly.

This study provides important insights for vegetation management and policy development. Policies should be optimized based on the underlying mechanisms of vegetation dynamics. To cope with future pressures from climate change and human disturbances, a sustained ecological investment mechanism should be established in ecologically fragile areas. Additionally, region-specific management strategies should be implemented, taking into account local climatic and elevational characteristics. Strengthened monitoring of human activities such as grazing, tourism, and road construction is also essential to mitigate their negative impacts. Moreover, improving ecological compensation mechanisms will be crucial for promoting vegetation restoration and ecosystem sustainability. Nevertheless, the coupled driving mechanisms of multiple factors on vegetation change, as well as the simulation of future vegetation dynamics, remain key directions for future research. Future studies should enhance the analysis of multi-factor interactions, explore their integrated effects on vegetation dynamics, and incorporate

high-resolution climate models and remote sensing technologies. Process-based ecological models and scenario simulations should be employed to predict vegetation changes under different conditions, particularly focusing on the overlay effects of natural and anthropogenic drivers, in order to further refine the knowledge system for vegetation dynamics management.

CRediT authorship contribution statement

Dazhi Yang: Writing – original draft, Visualization, Validation, Software, Methodology, Formal analysis. **Yaqun Liu:** Writing – review & editing, Supervision, Resources, Project administration, Investigation, Funding acquisition, Data curation, Conceptualization.

Declaration of competing interest

The authors declare that they have no known competing financial interests or personal relationships that could have appeared to influence the work reported in this paper.

Acknowledgments

This research was supported by the National Natural Science Foundation of China (Grant Nos. 42201289 and 42293270), the Strategic Priority Research Program of Chinese Academy of Sciences (Grant No. XDA20040301), and the Second Tibetan Plateau Scientific Expedition and Research (Grant No. 2019QZKK0603).

Data availability

All the data used have been explained in the manuscript.

References

- Adeyeri, O.E., Zhou, W., Ndehedehe, C.E., Wang, X., 2024. Global vegetation, moisture, thermal and climate interactions intensify compound extreme events. *Sci. Total Environ.* 912, 169261. <https://doi.org/10.1016/j.scitotenv.2023.169261>.
- Anees, S.A., Mehmood, K., Rehman, A., Rehman, N.U., Muhammad, S., Shahzad, F., Hussain, K., Luo, M., Alarfaj, A.A., Alharbi, S.A., Khan, W.R., 2024. Unveiling fractional vegetation cover dynamics: a spatiotemporal analysis using MODIS NDVI and machine learning. *Environmental and Sustainability Indicators* 24, 100485. <https://doi.org/10.1016/j.indic.2024.100485>.
- Augustine, D.J., Derner, J.D., Fernández-Giménez, M.E., Porensky, L.M., Wilmer, H., Briske, D.D., 2020. Adaptive, multipaddock rotational grazing management: a ranch-scale assessment of effects on vegetation and livestock performance in semiarid rangeland. *Rangel. Ecol. Manag.* 73, 796–810. <https://doi.org/10.1016/j.rama.2020.07.005>.
- Bagnara, M., Silveyra Gonzalez, R., Reifenberg, S., Steinkamp, J., Hickler, T., Werner, C., Dormann, C.F., Hartig, F., 2019. An R package facilitating sensitivity analysis, calibration and forward simulations with the LPJ-GUESS dynamic vegetation model. *Environ. Model. Software* 111, 55–60. <https://doi.org/10.1016/j.envsoft.2018.09.004>.
- Cavender-Bares, J., Schneider, F.D., Santos, M.J., Armstrong, A., Carnaval, A., Dahlin, K. M., Fatoyinbo, L., Hurt, G.C., Schimel, D., Townsend, P.A., Ustin, S.L., Wang, Z., Wilson, A.M., 2022. Integrating remote sensing with ecology and evolution to advance biodiversity conservation. *Nature Ecology & Evolution* 6, 506–519. <https://doi.org/10.1038/s41559-022-01702-5>.
- Chen, Y., Zhang, T., Zhu, X., Yi, G., Li, J., Bie, X., Hu, J., Liu, X., 2024. Quantitatively analyzing the driving factors of vegetation change in China: climate change and human activities. *Ecol. Inform.* 82, 102667. <https://doi.org/10.1016/j.ecoinf.2024.102667>.
- CMDSC, 2024. China meteorological data service centre. <https://data.cma.cn/en/> (accessed on November 1st, 2024).
- Degen, A.A., 2025. Chapter 17 - the impact of management and livestock grazing on the grasslands of the Qinghai-Tibetan Plateau. In: Shang, Z., Degen, A.A., Dong, S., et al. (Eds.), *Grassland Degradation, Restoration and Sustainable Management of Global Alpine Area*. Elsevier, pp. 379–402.
- Dobšinská, Z., Báliková, K., Jarský, V., Hrbáč, M., Štífil, R., Šálka, J., 2024. Evaluation analysis of the compensation payments schemes for ecosystem services: the case of Czech and Slovak Republic. *For. Pol. Econ.* 163, 103202. <https://doi.org/10.1016/j.forpol.2024.103202>.
- Ehlers, T.A., Chen, D., Appel, E., Bolch, T., Chen, F., Diekmann, B., Dippold, M.A., Giese, M., Guggenberger, G., Lai, H.-W., Li, X., Liu, J., Liu, Y., Ma, Y., Miche, G., Mosbrugger, V., Mulch, A., Piao, S., Schwab, A., et al., 2022. Past, present, and future geo-biosphere interactions on the Tibetan Plateau and implications for permafrost. *Earth Sci. Rev.* 234, 104197. <https://doi.org/10.1016/j.earscirev.2022.104197>.
- Ehrlich, D., Kemper, T., Pesaresi, M., Corbane, C., 2018. Built-up area and population density: two essential societal variables to address climate hazard impact. *Environ. Sci. Pol.* 90, 73–82. <https://doi.org/10.1016/j.envsci.2018.10.001>.
- Fathollahi, L., Wu, F., Melaki, R., Jamshidi, P., Sarwar, S., 2024. Global normalized difference vegetation index forecasting from air temperature, soil moisture and precipitation using a deep neural network. *Applied Computing and Geosciences* 23, 100174. <https://doi.org/10.1016/j.acags.2024.100174>.
- Fensholt, R., Sandholt, I., Rasmussen, M.S., 2004. Evaluation of MODIS LAI, FAPAR and the relation between FAPAR and NDVI in a semi-arid environment using in situ measurements. *Rem. Sens. Environ.* 91, 490–507. <https://doi.org/10.1016/j.rse.2004.04.009>.
- Forzieri, G., Alkama, R., Miralles, D.G., Cescatti, A., 2017. Satellites reveal contrasting responses of regional climate to the widespread greening of Earth. *Science* 356, 1180–1184. <https://doi.org/10.1126/science.aal1727>.
- Giglio, L., Boschetti, L., Roy, D.P., Humber, M.L., Justice, C.O., 2018. The collection 6 MODIS burned area mapping algorithm and product. *Rem. Sens. Environ.* 217, 72–85. <https://doi.org/10.1016/j.rse.2018.08.005>.
- Gocić, M., Trajković, S., 2013. Analysis of changes in meteorological variables using mann-kendall and Sen's slope estimator statistical tests in Serbia. *Global Planet. Change* 100, 172–182. <https://doi.org/10.1016/j.gloplacha.2012.10.014>.
- Güçlü, Y.S., 2018. Multiple Sen-innovative trend analyses and partial Mann-Kendall test. *J. Hydrol.* 566, 685–704. <https://doi.org/10.1016/j.jhydrol.2018.09.034>.
- Guo, K., Niu, X., Wang, B., 2023. A GIS-based study on the layout of the ecological monitoring system of the grain for green project in China. *Forests* 14, 70.
- Gutiérrez-Hernández, O., García, L.V., 2025. Uncovering true significant trends in global greening. *Remote Sens. Appl.: Society and Environment* 37, 101377. <https://doi.org/10.1016/j.rsase.2024.101377>.
- Hamed, K.H., 2009. Exact distribution of the mann-kendall trend test statistic for persistent data. *J. Hydrol.* 365, 86–94. <https://doi.org/10.1016/j.jhydrol.2008.11.024>.
- Han, Z., Song, W., 2022. Interannual trends of vegetation and responses to climate change and human activities in the great mekong subregion. *Global Ecology and Conservation* 38, e02215. <https://doi.org/10.1016/j.gecco.2022.e02215>.
- Idusueri, E.O., Awoniran, D.R., Izunobi, J.U., Abdulsheesh, T.H., Abbas, I.I., Olawole, M. O., 2024. Sustainable development goals, governance and assessment of the impact of urban growth on vegetation cover in Benin City, Nigeria, using land-use-land-cover change trajectories. *Discover Sustainability* 5, 291. <https://doi.org/10.1007/s43621-024-00508-8>.
- Jeong, S., Ryu, Y., Gentile, P., Lian, X., Fang, J., Li, X., Dechant, B., Kong, J., Choi, W., Jiang, C., Keenan, T.F., Harrison, S.P., Prentice, I.C., 2024. Persistent global greening over the last four decades using novel long-term vegetation index data with enhanced temporal consistency. *Rem. Sens. Environ.* 311, 114282. <https://doi.org/10.1016/j.rse.2024.114282>.
- Jia, Q., Gao, X., Jiang, Z., Li, H., Guo, J., Lu, X., Yonghong Li, F., 2024. Sensitivity of temperate vegetation to precipitation is higher in steppes than in deserts and forests. *Ecol. Indic.* 166, 112317. <https://doi.org/10.1016/j.ecolind.2024.112317>.
- Kemper, J., Renold, U., 2024. Evaluating the impact of general versus vocational education on labor market outcomes in Egypt by means of a regression discontinuity design. *J. Dev. Econ.* 166, 103172. <https://doi.org/10.1016/j.jdeveco.2023.103172>.
- Khormizi, H.Z., Ghafarian Malamiri, H.R., Alian, S., Stein, A., Kalantari, Z., Ferreira, C.S. S., 2023. Proof of evidence of changes in global terrestrial biomes using historic and recent NDVI time series. *Heliyon* 9, e18686. <https://doi.org/10.1016/j.heliyon.2023.e18686>.
- Kocev, D., Džeroski, S., White, M.D., Newell, G.R., Griffioen, P., 2009. Using single- and multi-target regression trees and ensembles to model a compound index of vegetation condition. *Ecol. Model.* 220, 1159–1168. <https://doi.org/10.1016/j.ecolmodel.2009.01.037>.
- Lavagnini, I., Badocco, D., Pastore, P., Magno, F., 2011. Theil-Sen nonparametric regression technique on univariate calibration, inverse regression and detection limits. *Talanta* 87, 180–188. <https://doi.org/10.1016/j.talanta.2011.09.059>.
- Li, S., Wang, G., Zhu, C., Lu, J., Ullah, W., Fifi Tawia Hagan, D., Kattel, G., Liu, Y., Zhang, Z., Song, Y., Sun, S., Zheng, Y., Peng, J., 2023. Vegetation growth due to CO₂ fertilization is threatened by increasing vapor pressure deficit. *J. Hydrol.* 619, 129292. <https://doi.org/10.1016/j.jhydrol.2023.129292>.
- Li, S., Zhang, H., Zhou, X., Yu, H., Li, W., 2020. Enhancing protected areas for biodiversity and ecosystem services in the Qinghai-Tibet Plateau. *Ecosyst. Serv.* 43, 101090. <https://doi.org/10.1016/j.ecoserv.2020.101090>.
- Li, S., Zhang, X., Lu, Z., Ni, J., Lu, J., 2024. Progress of vegetation modelling and future research prospects. *Sci. China Earth Sci.* 67, 2718–2738. <https://doi.org/10.1007/s11430-023-1367-1>.
- Li, W., Li, X., Tan, M., Wang, Y., 2017. Influences of population pressure change on vegetation greenness in China's mountainous areas. *Ecol. Evol.* 7, 9041–9053. <https://doi.org/10.1002/ece3.3424>.
- Li, X., Guo, H., Cheng, G., Song, X., Ran, Y., Feng, M., Che, T., Li, X., Wang, L., Duan, A., Shangguan, D., Chen, D., Jin, R., Deng, J., Su, J., Cao, B., 2025. Polar regions are critical in achieving global sustainable development goals. *Nat. Commun.* 16, 3879. <https://doi.org/10.1038/s41467-025-59178-3>.
- Liu, H., Liu, S., Wang, F., Liu, Y., Yu, L., Wang, Q., Sun, Y., Li, M., Sun, J., Han, Z., 2022. Management practices should be strengthened in high potential vegetation productivity areas based on vegetation phenology assessment on the Qinghai-Tibet Plateau. *Ecol. Indic.* 140, 108991. <https://doi.org/10.1016/j.ecolind.2022.108991>.
- Liu, Q., Yao, F., Garcia-Garcia, A., Zhang, J., Li, J., Ma, S., Li, S., Peng, J., 2023. The response and sensitivity of global vegetation to water stress: a comparison of

- different satellite-based NDVI products. *Int. J. Appl. Earth Obs. Geoinf.* 120, 103341. <https://doi.org/10.1016/j.jag.2023.103341>.
- Liu, Y., Li, Y., Li, S., Motesharrei, S., 2015. Spatial and temporal patterns of global NDVI trends: correlations with climate and human factors. *Remote Sens.* 7, 13233–13250.
- Lu, C., Zhang, Q., Woolway, R.I., Ma, L., Liu, T., Wang, G., Sun, D., Singh, V.P., Bai, Y., Sun, B., Huang, X., 2025. Global warming will increase the risk of water shortage in northwest China. *Earths Future* 13, e2025EF006199. <https://doi.org/10.1029/2025EF006199>.
- Lu, H.-L., Li, F.-F., Gong, T.-L., Gao, Y.-H., Li, J.-F., Qiu, J., 2023a. Reasons behind seasonal and monthly precipitation variability in the Qinghai-Tibet Plateau and its surrounding areas during 1979–2017. *J. Hydrol.* 619, 129329. <https://doi.org/10.1016/j.jhydrol.2023.129329>.
- Lu, H.-L., Li, F.-F., Gong, T.-L., Gao, Y.-H., Li, J.-F., Wang, G.-Q., Qiu, J., 2023b. Temporal variability of precipitation over the Qinghai-Tibetan Plateau and its surrounding areas in the last 40 years. *Int. J. Climatol.* 43, 1912–1934. <https://doi.org/10.1002/joc.7953>.
- Lu, H., Qiu, J., Hu, B.X., Li, F., 2024. Potential impact of precipitation temporal structure on meteorological drought and vegetation condition: a case study on Qinghai-Tibet Plateau. *J. Hydrol.: Reg. Stud.* 56, 102048. <https://doi.org/10.1016/j.ejrh.2024.102048>.
- Mann, H.B., 1945. Nonparametric tests against trend. *Econometrica* 13, 245–259. <https://doi.org/10.2307/1907187>.
- McNicol, I.M., Keane, A., Burgess, N.D., Bowers, S.J., Mitchard, E.T.A., Ryan, C.M., 2023. Protected areas reduce deforestation and degradation and enhance woody growth across African woodlands. *Commun. Earth Environ.* 4, 392. <https://doi.org/10.1038/s43247-023-01053-4>.
- Miao, C., Immerzeel, W.W., Xu, B., Yang, K., Duan, Q., Li, X., 2024. Understanding the Asian water tower requires a redesigned precipitation observation strategy. *Proc. Natl. Acad. Sci.* 121, e2403557121. <https://doi.org/10.1073/pnas.2403557121>.
- Mu, H., Li, X., Wen, Y., Huang, J., Du, P., Su, W., Miao, S., Geng, M., 2022. A global record of annual terrestrial human footprint dataset from 2000 to 2018. *Sci. Data* 9, 176. <https://doi.org/10.1038/s41597-022-01284-8>.
- NASA, 2015. ASTER global digital elevation model V003. In: NASA EOSDIS Land Processes Distributed Active Archive Center, pp. 1–13. <https://doi.org/10.5067/ASTER/ASTGTM.003>.
- OSM, 2019. OpenStreetMap. <https://www.openstreetmap.org>. (accessed on November 1st, 2024). Licensed under the Open Data Commons Open Database License (ODbL).
- Pan, N., Feng, X., Fu, B., Wang, S., Ji, F., Pan, S., 2018. Increasing global vegetation browning hidden in overall vegetation greening: insights from time-varying trends. *Rem. Sens. Environ.* 214, 59–72. <https://doi.org/10.1016/j.rse.2018.05.018>.
- Pang, G., Wang, X., Yang, M., 2017. Using the NDVI to identify variations in, and responses of, vegetation to climate change on the Tibetan Plateau from 1982 to 2012. *Quat. Int.* 444, 87–96. <https://doi.org/10.1016/j.quaint.2016.08.038>.
- Panigrahi, S., Verma, K., Tripathi, P., 2021. 12 - review of MODIS EVI and NDVI data for data mining applications. In: Thwel, T.T., Sinha, G.R. (Eds.), *Data Deduplication Approaches*. Academic Press, pp. 231–253.
- Peng, S.-S., Piao, S., Zeng, Z., Ciais, P., Zhou, L., Li, L.Z.X., Myneni, R.B., Yin, Y., Zeng, H., 2014. Afforestation in China cools local land surface temperature. *Proc. Natl. Acad. Sci.* 111, 2915–2919. <https://doi.org/10.1073/pnas.1315126111>.
- Piao, S., Tan, K., Nan, H., Ciais, P., Fang, J., Wang, T., Vuichard, N., Zhu, B., 2012. Impacts of climate and CO₂ changes on the vegetation growth and carbon balance of Qinghai-Tibetan grasslands over the past five decades. *Global Planet. Change* 98–99, 73–80. <https://doi.org/10.1016/j.gloplacha.2012.08.009>.
- Piao, S., Wang, X., Park, T., Chen, C., Lian, X., He, Y., Bjerke, J.W., Chen, A., Ciais, P., Tømmervik, H., Nemani, R.R., Myneni, R.B., 2020. Characteristics, drivers and feedbacks of global greening. *Nat. Rev. Earth Environ.* 1, 14–27. <https://doi.org/10.1038/s43017-019-0001-x>.
- Pontes-Lopes, A., Silva, C.V.J., Barlow, J., Rincón, L.M., Campanharo, W.A., Nunes, C.A., de Almeida, C.T., Silva Júnior, C.H.L., Cassol, H.L.G., Dalagnol, R., Stark, S.C., Graça, P.M.L.A., Aragão, L.E.O.C., 2021. Drought-driven wildfire impacts on structure and dynamics in a wet central Amazonian forest. *Proc. Biol. Sci.* 288, 20210094. <https://doi.org/10.1098/rspb.2021.0094>.
- PRC, 2023. People's Republic of China (PRC) Qinghai-Tibet Plateau ecological protection law. The State Council, The People's Government of the People's Republic of China. https://www.gov.cn/yaowen/2023-04/27/content_5753376.htm (accessed on November 1st, 2024).
- Qi, G., Cong, N., Qiu, T., Rong, L., Ren, P., Xiao, J., 2025. Evaluation of impact of climate extremes on vegetation change in southwest China considering time-lag effect. *Global Ecology and Conservation* 58, e03497. <https://doi.org/10.1016/j.gecco.2025.e03497>.
- Recuero, L., Litago, J., Pinzón, J.E., Huesca, M., Moyano, M.C., Palacios-Orueta, A., 2019. Mapping periodic patterns of global vegetation based on spectral analysis of NDVI time series. *Remote Sens.* 11, 2497.
- RESDP, 2024. Resource and environmental science data platform. <https://www.resdp.cn/>.(accessed on November 1st, 2024).
- Rogier, d.J., Sytze, d.B., Allard, d.W., Michael, E., David L, D., 2011. Analysis of monotonic greening and browning trends from global NDVI time-series. *Rem. Sens. Environ.* 115, 692–702. <https://doi.org/10.1016/j.rse.2010.10.011>.
- Shao, Q., Liu, S., Ning, J., Liu, G., Yang, F., Zhang, X., Niu, L., Huang, H., Fan, J., Liu, J., 2022. Assessment of ecological benefits of key national ecological projects in China in 2000–2019 using remote sensing. *Acta Geogr. Sin.* 77, 2133–2153. <https://doi.org/10.11821/dlx202209001>.
- Shen, F., Yang, L., Zhang, L., Guo, M., Huang, H., Zhou, C., 2023. Quantifying the direct effects of long-term dynamic land use intensity on vegetation change and its interacted effects with economic development and climate change in Jiangsu, China. *J. Environ. Manag.* 325, 116562. <https://doi.org/10.1016/j.jenvman.2022.116562>.
- Shen, M., Piao, S., Jeong, S.-J., Zhou, L., Zeng, Z., Ciais, P., Chen, D., Huang, M., Jin, C.-S., Li, L.Z.X., Li, Y., Myneni, R.B., Yang, K., Zhang, G., Zhang, Y., Yao, T., 2015. Evaporative cooling over the Tibetan Plateau induced by vegetation growth. *Proc. Natl. Acad. Sci.* 112, 9299–9304. <https://doi.org/10.1073/pnas.1504418112>.
- Song, W., Feng, Y., Wang, Z., 2022. Ecological restoration programs dominate vegetation greening in China. *Sci. Total Environ.* 848, 157729. <https://doi.org/10.1016/j.scitotenv.2022.157729>.
- Sun, L., Li, H., Wang, J., Chen, Y., Xiong, N., Wang, Z., Wang, J., Xu, J., 2023. Impacts of climate change and human activities on NDVI in the Qinghai-Tibet Plateau. *Remote Sens.* 15, 587.
- Sun, Y., Liu, S., Liu, Y., Dong, Y., Li, M., An, Y., Shi, F., 2022. Grazing intensity and human activity intensity data sets on the Qinghai-Tibetan Plateau during 1990–2015. *Geoscience Data Journal* 9, 140–153. <https://doi.org/10.1002/gdj3.127>.
- Thompson, N., Salzmann, U., Hutchinson, D.K., Strother, S.L., Pound, M.J., Utescher, T., Brugger, J., Hickler, T., Hocking, E.P., Lunt, D.J., 2025. Global vegetation zonation and terrestrial climate of the warm early Eocene. *Earth Sci. Rev.* 261, 105036. <https://doi.org/10.1016/j.earscirev.2024.105036>.
- Tortini, R., van Manen, S.M., Parkes, B.R.B., Carn, S.A., 2017. The impact of persistent volcanic degassing on vegetation: a case study at Turrialba volcano, Costa Rica. *Int. J. Appl. Earth Obs. Geoinf.* 59, 92–103. <https://doi.org/10.1016/j.jag.2017.03.002>.
- TPDC, 2024. Qinghai-Tibet Plateau scientific data center. <https://data.tpdc.ac.cn/home>. (accessed on April 1st, 2025).
- USGS, 2020. Terra moderate resolution imaging spectroradiometer (MODIS) vegetation indices monthly (MOD13A3) version 6.1 data. NASA EOSDIS Land Processes Distributed Active Archive Center. <https://doi.org/10.5067/MODIS/MOD13A3.061>.
- Wang, D., Peng, Q., Li, X., Zhang, W., Xia, X., Qin, Z., Ren, P., Liang, S., Yuan, W., 2024. A long-term high-resolution dataset of grasslands grazing intensity in China. *Sci. Data* 11, 1194. <https://doi.org/10.1038/s41597-024-04045-x>.
- Wang, G., Bai, W., Li, N., Hu, H., 2011. Climate changes and its impact on tundra ecosystem in Qinghai-Tibet Plateau. *China. Climatic Change* 106, 463–482. <https://doi.org/10.1002/s10584-010-9952-0>.
- Wang, H., Liu, H., Huang, N., Bi, J., Ma, X., Ma, Z., Shangguan, Z., Zhao, H., Feng, Q., Liang, T., Cao, G., Schmid, B., He, J.-S., 2021. Satellite-derived NDVI underestimates the advancement of alpine vegetation growth over the past three decades. *Ecology* 102, e03518. <https://doi.org/10.1002/ecy.3518>.
- Wang, S., Zhang, Y., Ju, W., Chen, J.M., Cias, P., Cescatti, A., Sardans, J., Janssens, I.A., Wu, M., Berry, J.A., Campbell, E., Fernández-Martínez, M., Alkama, R., Sitch, S., Friedlingstein, P., Smith, W.K., Yuan, W., He, W., Lombardozzi, D., et al., 2020. Recent global decline of CO₂ fertilization effects on vegetation photosynthesis. *Science* 370, 1295–1300. <https://doi.org/10.1126/science.abb7772>.
- Wei, Y., Lu, H., Wang, J., Wang, X., Sun, J., 2022. Dual influence of climate change and anthropogenic activities on the spatiotemporal vegetation dynamics over the Qinghai-Tibetan Plateau from 1981 to 2015. *Earths Future* 10, e2021EF002566. <https://doi.org/10.1029/2021EF002566>.
- Wellmann, T., Schug, F., Haase, D., Pfleiderer, D., van der Linden, S., 2020. Green growth? On the relation between population density, land use and vegetation cover fractions in a city using a 30-years landsat time series. *Landsc. Urban Plann.* 202, 103857. <https://doi.org/10.1016/j.landurbplan.2020.103857>.
- Wen, Z., Wu, S., Chen, J., Lü, M., 2017. NDVI indicated long-term interannual changes in vegetation activities and their responses to climatic and anthropogenic factors in the three gorges reservoir region, China. *Sci. Total Environ.* 574, 947–959. <https://doi.org/10.1016/j.scitotenv.2016.09.049>.
- Werner, R., Valev, D., Danov, D., Guineva, V., 2015. Study of structural break points in global and hemispheric temperature series by piecewise regression. *Adv. Space Res.* 56, 2323–2334. <https://doi.org/10.1016/j.asr.2015.09.007>.
- WorldPop, 2019. WorldPop hub. <https://hub.worldpop.org/geodata/listing?id=74>. (accessed on November 1st, 2024). Licensed under the Creative Commons Attribution 4.0 International License (CC BY 4.0).
- Wu, D., Zhao, X., Liang, S., Zhou, T., Huang, K., Tang, B., Zhao, W., 2015. Time-lag effects of global vegetation responses to climate change. *Glob. Change Biol.* 21, 3520–3531. <https://doi.org/10.1111/gcb.12945>.
- Wu, G., Zhou, X., Xu, X., Huang, J., Duan, A., Yang, S., Hu, W., Ma, Y., Liu, Y., Bian, J., Fu, Y., Yang, H., Zhao, P., Zhong, L., Ma, W., 2023. An integrated research plan for the Tibetan Plateau land-air coupled system and its impacts on the global climate. *Bull. Am. Meteorol. Soc.* 104, E158–E177. <https://doi.org/10.1175/BAMS-D-21-0293.1>.
- Xiao, J., Xie, B., Zhou, K., Liang, C., Li, J., Xie, J., Zhang, X., 2023. Bidirectional dependency between vegetation and terrestrial water storage in China. *J. Hydrol.* 626, 130313. <https://doi.org/10.1016/j.jhydrol.2023.130313>.
- Yan, Y., Mao, K., Shen, X., Cao, M., Xu, T., Guo, Z., Bao, Q., 2021. Evaluation of the influence of ENSO on tropical vegetation in long time series using a new indicator. *Ecol. Indic.* 129, 107872. <https://doi.org/10.1016/j.ecolind.2021.107872>.
- Yan, Y., Piao, S., Hammond, W.M., Chen, A., Hong, S., Xu, H., Munson, S.M., Myneni, R.B., Allen, C.D., 2024. Climate-induced tree-mortality pulses are obscured by broad-scale and long-term greening. *Nature Ecology & Evolution* 8, 912–923. <https://doi.org/10.1038/s41559-024-02372-1>.
- Yang, X., Li, X., Wang, X., Ding, F., Chen, F., Wang, J., Zhang, X., Zhang, Y., 2022. Meta-analysis of the correlation between vegetation and precipitation in the temperate deserts of the northern Hemisphere over the last 40 years. *Ecol. Indic.* 142, 109269. <https://doi.org/10.1016/j.ecolind.2022.109269>.
- Yang, Y., Wang, X., Wang, T., 2024. Permafrost degradation induces the abrupt changes of vegetation NDVI in the Northern hemisphere. *Earths Future* 12, e2023EF004309. <https://doi.org/10.1029/2023EF004309>.
- Yao, T., Bolch, T., Chen, D., Gao, J., Immerzeel, W., Piao, S., Su, F., Thompson, L., Wada, Y., Wang, L., Wang, T., Wu, G., Xu, B., Yang, W., Zhang, G., Zhao, P., 2022.

- The imbalance of the Asian water tower. *Nat. Rev. Earth Environ.* 3, 618–632. <https://doi.org/10.1038/s43017-022-00299-4>.
- Yao, T., Xue, Y., Chen, D., Chen, F., Thompson, L., Cui, P., Koike, T., Lau, W.K.-M., Lettenmaier, D., Mosbrugger, V., Zhang, R., Xu, B., Dozier, J., Gillespie, T., Gu, Y., Kang, S., Piao, S., Sugimoto, S., Ueno, K., et al., 2019. Recent third pole's rapid warming accompanies cryospheric melt and water cycle intensification and interactions between monsoon and environment: multidisciplinary approach with observations, modeling, and analysis. *Bull. Am. Meteorol. Soc.* 100, 423–444. <https://doi.org/10.1175/BAMS-D-17-0057.1>.
- You, Q., Cai, Z., Pepin, N., Chen, D., Ahrens, B., Jiang, Z., Wu, F., Kang, S., Zhang, R., Wu, T., Wang, P., Li, M., Zuo, Z., Gao, Y., Zhai, P., Zhang, Y., 2021. Warming amplification over the Arctic Pole and Third Pole: trends, mechanisms and consequences. *Earth Sci. Rev.* 217, 103625. <https://doi.org/10.1016/j.earscirev.2021.103625>.
- Yu, H., Xiao, H., Gu, X., 2024. Integrating species distribution and piecewise linear regression model to identify functional connectivity thresholds to delimit urban ecological corridors. *Comput. Environ. Urban Syst.* 113, 102177. <https://doi.org/10.1016/j.compenvurbsys.2024.102177>.
- Yu, W., Liu, Y., Xu, L., Wu, G., Yang, S., Chen, D., Yang, X.-Q., Hu, C., He, B., 2022. Potential impact of Spring thermal forcing over the Tibetan Plateau on the following Winter El Niño–southern oscillation. *Geophys. Res. Lett.* 49, e2021GL097234. <https://doi.org/10.1029/2021GL097234>.
- Zarei, A., Madani, K., Guenther, E., Nasrabadi, H.M., Hoff, H., 2024. Integrated nexus approach to assessing climate change impacts on grassland ecosystem dynamics: a case study of the grasslands in Tanzania. *Sci. Total Environ.* 952, 175691. <https://doi.org/10.1016/j.scitotenv.2024.175691>.
- Zhang, C., Willis, C.G., Klein, J.A., Ma, Z., Li, J., Zhou, H., Zhao, X., 2017a. Recovery of plant species diversity during long-term experimental warming of a species-rich alpine meadow community on the Qinghai-Tibet plateau. *Biol. Conserv.* 213, 218–224. <https://doi.org/10.1016/j.biocon.2017.07.019>.
- Zhang, H., Fan, J., Wang, J., Cao, W., Harris, W., 2018. Spatial and temporal variability of grassland yield and its response to climate change and anthropogenic activities on the Tibetan Plateau from 1988 to 2013. *Ecol. Indic.* 95, 141–151. <https://doi.org/10.1016/j.ecolind.2018.05.088>.
- Zhang, L., Shen, M., Jiang, N., Lv, J., Liu, L., Zhang, L., 2023. Spatial variations in the response of spring onset of photosynthesis of evergreen vegetation to climate factors across the Tibetan Plateau: the roles of interactions between temperature, precipitation, and solar radiation. *Agric. For. Meteorol.* 335, 109440. <https://doi.org/10.1016/j.agrformet.2023.109440>.
- Zhang, S., Zhou, L., Zhang, L., Yang, Y., Wei, Z., Zhou, S., Yang, D., Yang, X., Wu, X., Zhang, Y., Li, X., Dai, Y., 2022. Reconciling disagreement on global river flood changes in a warming climate. *Nat. Clim. Change* 12, 1160–1167. <https://doi.org/10.1038/s41558-022-01539-7>.
- Zhang, Y., Song, C., Band, L.E., Sun, G., Li, J., 2017b. Reanalysis of global terrestrial vegetation trends from MODIS products: browning or greening? *Rem. Sens. Environ.* 191, 145–155. <https://doi.org/10.1016/j.rse.2016.12.018>.
- Zhou, H., Qiu, J., Li, M., Lu, H., Li, F., 2025. Assessment of large-scale reservoirs' impact on the local precipitation. *Water Resour. Res.* 61, e2025WR039938. <https://doi.org/10.1029/2025WR039938>.
- Zhou, J., Niu, J., Wu, N., Lu, T., 2024. Annual high-resolution grazing-intensity maps on the Qinghai–Tibet Plateau from 1990 to 2020. *Earth Syst. Sci. Data* 16, 5171–5189. <https://doi.org/10.5194/essd-16-5171-2024>.
- Zhu, Q., Chen, H., Peng, C., Liu, J., Piao, S., He, J.-S., Wang, S., Zhao, X., Zhang, J., Fang, X., Jin, J., Yang, Q.-E., Ren, L., Wang, Y., 2023. An early warning signal for grassland degradation on the Qinghai-Tibetan Plateau. *Nat. Commun.* 14, 6406. <https://doi.org/10.1038/s41467-023-42099-4>.